

Assessment of model estimates of land–atmosphere CO₂ exchange across Northern Eurasia

M. A. Rawlins¹, A. D. McGuire², J. K. Kimball³, P. Dass¹, D. Lawrence⁴,
E. Burke⁵, X. Chen⁶, C. Delire⁷, C. Koven⁸, A. MacDougall⁹, S. Peng^{10,15},
A. Rinke^{11,12}, K. Saito¹³, W. Zhang¹⁴, R. Alkama⁷, T. J. Bohn¹⁵, P. Ciais¹⁰,
B. Decharme⁷, I. Gouttevin^{16,17}, T. Hajima¹³, D. Ji¹¹, G. Krinner¹⁶,
D. P. Lettenmaier¹⁸, P. Miller¹⁴, J. C. Moore¹¹, B. Smith¹⁴, and T. Sueyoshi¹³

¹Climate System Research Center, Department of Geosciences, University of Massachusetts, Amherst, MA, USA

²U.S. Geological Survey, Alaska Cooperative Fish and Wildlife Research Unit, University of Alaska, Fairbanks, Alaska, USA

³FLBS/NTSG, Univ. of Montana, Missoula, MT, USA

⁴National Center for Atmospheric Research, Boulder, CO, USA

⁵Met Office Hadley Centre, FitzRoy Road, Exeter, EX1 3PB, UK

⁶Department of Civil and Environmental Engineering, University of Washington, Seattle, WA, USA

⁷CRNM-GAME, Unité mixte de recherche CNRS/Meteo-France (UMR 3589), 42 av Coriolis, 31057 Toulouse CEDEX, France

Title Page

Abstract

Introduction

Conclusions

References

Tables

Figures



Back

Close

Full Screen / Esc

Printer-friendly Version

Interactive Discussion



⁸Lawrence Berkeley National Laboratory, Berkeley, CA, USA

⁹School of Earth and Ocean Sciences, University of Victoria, Victoria, BC, Canada

¹⁰Laboratoire des Sciences du Climat et de l'Environnement, CEA-CNRS-UVSQ, UMR8212, 91191 Gif-sur-Yvette, France

¹¹State Key Laboratory of Earth Surface Processes and Resource Ecology, College of Global Change and Earth System Science, Beijing Normal University, Beijing, China

¹²Alfred Wegener Institute, Helmholtz Centre for Polar and Marine Research, Potsdam, Germany

¹³Research Institute for Global Change, Japan Agency for Marine-Earth Science and Technology, Yokohama, Kanagawa, Japan

¹⁴Department of Physical Geography and Ecosystem Science, Lund University, Sölvegatan 12, 223 62 Lund, Sweden

¹⁵School of Earth and Space Exploration, Arizona State University, Tempe, AZ, USA

¹⁶UJF–Grenoble 1/CNRS, Laboratoire de Glaciologie et Géophysique de l'Environnement (LGGE), UMR 5183, BP53, 38041 Grenoble, France

¹⁷Irstea, UR HHLY, 5 rue de la Doua, CS 70077, 69626 Villeurbanne CEDEX, France

¹⁸Department of Geography, University of California, Los Angeles, CA, USA

Received: 8 January 2015 – Accepted: 21 January 2015 – Published: 3 February 2015

Correspondence to: M. A. Rawlins (rawlins@geo.umass.edu)

Published by Copernicus Publications on behalf of the European Geosciences Union.

BGD

12, 2257–2305, 2015

CO₂ exchange across Northern Eurasia

M. A. Rawlins et al.

Title Page

Abstract

Introduction

Conclusions

References

Tables

Figures

⏪

⏩

◀

▶

Back

Close

Full Screen / Esc

Printer-friendly Version

Interactive Discussion



Abstract

A warming climate is altering land–atmosphere exchanges of carbon, with a potential for increased vegetation productivity as well as the mobilization of permafrost soil carbon stores. Here we investigate land–atmosphere carbon dioxide (CO₂) dynamics through analysis of net ecosystem productivity (NEP) and its component fluxes of gross primary productivity (GPP) and ecosystem respiration (ER) and soil carbon residence time, simulated by a set of land surface models (LSMs) over a region spanning the drainage basin of northern Eurasia. The retrospective simulations were conducted over the 1960–2009 record and at 0.5° resolution, which is a scale common among many global carbon and climate model simulations. Model performance benchmarks were drawn from comparisons against both observed CO₂ fluxes derived from site-based eddy covariance measurements as well as regional-scale GPP estimates based on satellite remote sensing data. The site-based comparisons show the timing of peak GPP to be well simulated. Modest overestimates in model GPP and ER are also found, which are relatively higher for two boreal forest validation sites than the two tundra sites. Across the suite of model simulations, NEP increases by as little as 0.01 to as much as 0.79 g C m⁻² yr⁻², equivalent to 3 to 340 % of the respective model means, over the analysis period. For the multimodel average the increase is 135 % of the mean from the first to last ten years of record (1960–1969 vs 2000–2009), with a weakening CO₂ sink over the latter decades. Vegetation net primary productivity increased by 8 to 30 % from the first to last ten years, contributing to soil carbon storage gains, while model mean residence time for soil organic carbon decreased by 10 % (–5 to –16 %). This suggests that inputs to the soil carbon pool exceeded losses, resulting in a net gain amid a decrease in residence time. Our analysis points to improvements in model elements controlling vegetation productivity and soil respiration as being needed for reducing uncertainty in land–atmosphere CO₂ exchange. These advances require collection of new field data on vegetation and soil dynamics, the development of benchmarking datasets from measurements and remote sensing observations, and investments

BGD

12, 2257–2305, 2015

CO₂ exchange across Northern Eurasia

M. A. Rawlins et al.

Title Page

Abstract

Introduction

Conclusions

References

Tables

Figures

◀

▶

◀

▶

Back

Close

Full Screen / Esc

Printer-friendly Version

Interactive Discussion



in future model development and intercomparison studies. Resulting improvements in parameterizations and processes driving productivity and soil respiration rates will increase confidence in model estimates of net CO₂ exchange, component carbon fluxes, and underlying drivers of change across the northern high latitudes.

1 Introduction

The Arctic is believed to have been a net sink of carbon during the Holocene (Pries et al., 2012). Northern boreal regions play a considerable role in the land–atmosphere exchange of CO₂ at high latitudes (Graven et al., 2013), and during modern times, often referred to as the anthropocene (Crutzen, 2006), warming across the high northern latitudes has occurred at a faster rate than the rest of the globe, potentially through feedbacks involving biogeochemical and biogeophysical processes (Cox et al., 2000; Serreze and Barry, 2011). Warming may increase soil microbial decomposition, placing the large permafrost carbon pool at greater risk for being mobilized and transferred to the atmosphere as greenhouse gases (GHGs), thus providing a positive feedback to global climate (Dutta et al., 2006; Vogel et al., 2009; Schuur et al., 2009). Warming may also lead to longer growing seasons, contributing to increased plant productivity and ecosystem carbon sequestration (Melillo et al., 1993; Euskirchen et al., 2006). Satellite observations show broad greening trends in tundra regions (Myneni et al., 1997; Goetz et al., 2005; Zhang et al., 2008), suggesting a potential increase in the land sink of atmospheric CO₂. Some areas, however, are browning (Goetz et al., 2006).

There exists considerable uncertainty in contemporary magnitudes and temporal trends in land–atmosphere exchanges of CO₂. A recent synthesis of observations and models by McGuire et al. (2012) suggests that tundra regions across the pan-Arctic were a sink for atmospheric CO₂ and a source of CH₄ from 1990–2009. However a meta-analysis of 40 yr of CO₂ flux observations from 54 studies spanning 32 sites across northern high latitudes found that tundra was an annual CO₂ source from the mid-1980s until the 2000s, with the data suggesting an increase in winter respiration

Title Page

Abstract

Introduction

Conclusions

References

Tables

Figures



Back

Close

Full Screen / Esc

Printer-friendly Version

Interactive Discussion



**CO₂ exchange across
Northern Eurasia**

M. A. Rawlins et al.

Title Page

Abstract

Introduction

Conclusions

References

Tables

Figures

I ◀

▶ I

◀

▶

Back

Close

Full Screen / Esc

Printer-friendly Version

Interactive Discussion



rates, particularly over the last decade (Belshe et al., 2013). In an analysis of outputs from several models which have been part of recent terrestrial biosphere model intercomparison projects, Fisher et al. (2014) find that spatial patterns in carbon stocks and fluxes over Alaska varied widely, with some models showing a strong carbon sink, others a strong carbon source, and some showing the region as carbon neutral. It is critical to understand the net carbon sink as recent studies suggest that with continued warming the Arctic may transition from a net sink of atmospheric CO₂ to a net source over coming decades (Hayes et al., 2011; Koven et al., 2011; Schaefer et al., 2011; MacDougall et al., 2013; Oechel et al., 2014). In a study using a process model which included disturbances, Hayes et al. (2011) estimated a 73% reduction in the strength of the pan-Arctic land-based CO₂ sink over 1997–2006 vs. previous decades in the late 20th century.

Recent studies have provided new insights into model uncertainties relevant to our understanding of the land-based CO₂ sink across northern Eurasia. Quegan et al. (2011) examined several independent estimates of the carbon balance of Russia including two dynamic global vegetation models (DGVMs), two atmospheric inversion methods, and a landscape-ecosystem approach (LEA) incorporating observed data. They concluded that estimates of heterotrophic respiration were biased high in the two DGVMs and that the LEA appeared to give the most credible estimates of the fluxes. In an analysis of the terrestrial carbon budget of Russia using inventory-based, eddy covariance, and inversion methods, Dolman et al. (2012) noted good agreement in net ecosystem exchange among these bottom-up and top-down methods, estimating an average CO₂ sink across the three methods of 613.5 Tg C yr⁻¹. Their examination of outputs from a set of DGVMs, however, showed a much lower sink of 91 Tg C yr⁻¹. These analyses highlight the need for comprehensive assessments of numerical model estimates of spatial and temporal variations in land–atmosphere CO₂ exchange against independent data sources. A notable lack of direct flux measurements across northern land areas presents considerable challenges for model validation efforts (Fisher et al., 2014).

**CO₂ exchange across
Northern Eurasia**

M. A. Rawlins et al.

[Title Page](#)[Abstract](#)[Introduction](#)[Conclusions](#)[References](#)[Tables](#)[Figures](#)[I◀](#)[▶I](#)[◀](#)[▶](#)[Back](#)[Close](#)[Full Screen / Esc](#)[Printer-friendly Version](#)[Interactive Discussion](#)

In this study we examine model estimates of NEP and its component fluxes GPP and ER across northern Eurasia from a series of retrospective simulations for the period 1960–2009. Our analysis is unique in its synthesis of a large suite of sophisticated land-surface models, available site-level data, and a remote-sensing product. Study goals are two-fold. First, using the available in-situ data derived from tower-based measurements and the remote-sensing GPP product we seek to assess model efficacy in simulating spatial and temporal variations in GPP, ER, and NEP across the region. In doing so we elucidate issues complicating evaluations of model simulations of the carbon cycle across northern Eurasia and, by extension, other areas of the northern high latitudes. Second we estimate time changes in NEP and soil organic carbon (SOC) residence time and its controls as an indicator of climate sensitivity and potential vulnerability of soil carbon stocks across the region. We focus the analysis and discussion on assessing how well the models capture the seasonal cycle and spatial patterns in GPP and ER flux rates, evaluating uncertainties in the net CO₂ exchange given reported biases in respiration rates, and in advancing understanding of the cycling of CO₂ between the land and atmosphere over recent decades.

2 Methods

2.1 Study region

The spatial domain is the arctic drainage basin of northern Eurasia which comprises all land areas draining to the Arctic Ocean, a region of some 13.5 million km² (Fig. 1). The basin covers roughly half of the Northern Eurasian Earth Science Partnership Initiative (NEESPI) study area, loosely defined as the region between 15° E in the west, the Pacific Coast in the east, 40° N in the south, and the Arctic Ocean coastal zone in the north (Groisman et al., 2009). Warming and associated environmental changes to this region are among the most pronounced globally (Groisman and Bartalev, 2007; Groisman and Soja, 2009). Tundra vegetation is common across much of the higher

latitudes, with boreal forest and taiga vegetation comprising much of the remainder of the region. Steppes and grasslands are found across a relative small area in the extreme southwest. Continuous permafrost underlies over half of the region. Sporadic and relic permafrost comprise the southwest portion of the domain. West to east, the Ob, Yenese, Lena, and Kolyma rivers drain a large fraction of the total river discharge from the northern Eurasian basin.

2.2 Modeled data

We used outputs from retrospective simulations of nine models participating in the model integration group of the Permafrost Carbon Research Coordination Network (PCRCN). All simulation outputs available at the time of this writing were included in the analysis (<http://www.permafrostcarbon.org>, accessed 10 May 2014). The simulation protocol allowed for the choice of a model's driving datasets for atmospheric CO₂, N deposition, climate, disturbance, and other forcings. Simulations were run at daily or sub-daily time steps in some models and at 0.5° resolution over all land areas north of 45° N latitude. The present study focuses on analysis of spatial patterns and temporal changes in land-atmosphere CO₂ fluxes over the period 1960–2009. Quantities analyzed are GPP, ER, and NEP, defined here as $NEP = GPP - ER$, where a positive value represents a net sink of CO₂ into the ecosystem. ER is the sum of heterotrophic respiration and autotrophic respiration as estimated by the models. In this study we follow the conceptual framework for NEP and related terms as described in Chapin III et al. (2005). For the PCRCN modeling groups are providing gridded data for permafrost regions of the Northern Hemisphere. The nine models examined here (full model names in Table 1) are the (1) CLM version 4.5 (hereafter CLM4.5, Oleson et al., 2013); (2) CoLM (Dai et al., 2003, 2004); (3) ISBA (Decharme et al., 2011); (4) JULES (Best et al., 2011; Clark et al., 2011); (5) LPJ Guess WHyMe (hereafter LPJG, Smith et al., 2001; Wania et al., 2009a, b, 2010; Miller and Smith, 2012); (6) MIROC-ESM (Watanabe et al., 2011); (7) ORCHIDEE-IPSL (Koven et al., 2009, 2011; Gouttevin et al., 2012); (8) UVic (Avis et al., 2011; MacDougall et al., 2013); and (9) UW-VIC (Bohn

Title Page

Abstract

Introduction

Conclusions

References

Tables

Figures



Back

Close

Full Screen / Esc

Printer-friendly Version

Interactive Discussion



et al., 2013). Table 2 lists the model elements most closely related to CO₂ source and sink dynamics. These include model land cover initialization, time series forcings, light use efficiency, and CO₂ and nitrogen fertilization. The LPJG and MIROC are considered dynamic global vegetation models (DGVMs), wherein vegetation is allowed to change over the model simulation period. Among these models there exists a wide range of accounting for processes related to disturbances such as fire and land use change (Table 2). While studies that examine the overall ecosystem carbon balance (i.e. the net ecosystem carbon balance, NECB) are elemental to our understanding of the carbon cycle of northern Eurasia, the present study focuses on the patterns in NEP and component fluxes GPP and ER, common in all of the models, in order to avoid the uncertainties given the range of model formulations related to the full carbon balance. Outputs from several of the nine models have been examined in other recent studies. The LPJG and ORCHIDEE were used in the synthesis of data and models presented by McGuire et al. (2012). JULES, LPJG, ORCHIDEE, and CLM4.5 participated in the TRENDY MIP (Piao et al., 2013). CLM4.5, ORCHIDEE, and LPJG were three of the eight models examined in the study of Dolman et al. (2012). The nine models examined here have been used to characterize the relationship between air and near-surface soil temperatures in the Northern Hemisphere permafrost region (Rinke et al., 2014).

2.3 Observation data

2.3.1 Flux tower eddy covariance data

Model estimates for GPP, ER, and NEP are evaluated against data from four eddy covariance flux towers located across Russia and contained in the La Thuile global FLUXNET dataset (Baldocchi, 2008). FLUXNET represents a global network of tower eddy covariance measurement sites for monitoring land-atmosphere exchanges of carbon dioxide and water vapor (<http://daac.ornl.gov/FLUXNET/fluxnet.shtml>). Monthly GPP and ER are available for years 2002–2005. Observations during colder months are few. Tower sites are identified here by their locations: Chersky (CHE), Chokurdakh

BGD

12, 2257–2305, 2015

CO₂ exchange across Northern Eurasia

M. A. Rawlins et al.

Title Page

Abstract

Introduction

Conclusions

References

Tables

Figures

◀

▶

◀

▶

Back

Close

Full Screen / Esc

Printer-friendly Version

Interactive Discussion



(COK), Nur-Hakasija (HAK), and Zotino (ZOT). The first two (CHE and COK) are located in northeast Russia in the general zone of tundra vegetation and the remaining two sites (HAK and ZOT) are located in the boreal zone in the south-central part of the region (Fig. 1). Data are available for years 2002–2004 at Chersky, Nur-Hakasija and Zotino, and 2003–2005 at Chokurdakh. General characteristics of these sites are summarized in Table 3. In this dataset GPP and ER are derived from an empirical model driven by field-based eddy covariance measurements of net ecosystem CO₂ exchange (NEE) using methodologies described in Reichstein et al. (2005).

2.3.2 Satellite-based estimates of GPP

Satellite data driven estimates of annual total GPP are also obtained from the MODIS (Moderate Resolution Imaging Spectroradiometer) MOD17 operational product (Running et al., 2004; Zhao et al., 2005). The MOD17 product has been derived operationally from the NASA EOS MODIS sensors since 2000 and provides a globally consistent and continuous estimation of vegetation productivity at 1 km resolution and 8 day intervals. MOD17 uses a light use efficiency algorithm driven by global land cover classification and canopy fractional photosynthetically active radiation (FPAR) inputs from MODIS. The product also uses daily surface meteorology inputs from global re-analysis data (Zhao and Running, 2010), and land cover class specific biophysical response functions to estimate the conversion efficiency of canopy absorbed photosynthetically active radiation to vegetation biomass (g C MJ⁻¹) and GPP (Running et al., 2004). The MOD17 algorithms and productivity estimates have been extensively evaluated for a range of regional and global applications, including northern, boreal and Arctic domains. We use the MOD17 Collection 5 product, which has undergone five major reprocessing improvements since 2000. The MOD17 data are used in this study as a consistent satellite-derived baseline for evaluating GPP simulations from the detailed carbon process models.

BGD

12, 2257–2305, 2015

CO₂ exchange across Northern Eurasia

M. A. Rawlins et al.

Title Page

Abstract

Introduction

Conclusions

References

Tables

Figures

◀

▶

◀

▶

Back

Close

Full Screen / Esc

Printer-friendly Version

Interactive Discussion



3 Results

3.1 Model evaluation and benchmarking

3.1.1 Site-level evaluations

Confident assessments of uncertainties in land-atmosphere CO₂ fluxes is dependent on robust comparisons of model estimates against consistent benchmarking data. Monthly GPP from the models and MOD17 product are compared with cumulative monthly tower data by extracting the model values for the grid cell encompassing each tower site. MOD17 GPP agrees well with the tower-based estimates for Chersky and Chokurdakh (Fig. 2), with average errors over the three years of -2 and -11 gCm⁻²month⁻¹, respectively (Table 4). The comparisons show MOD17 GPP broadly agrees with the tower estimates at sites Nur-Hakasija and Zotino; average errors are 13 and 10 gCm⁻² month⁻¹, respectively, for these sites with higher productivity than Chersky and Chokurdakh. Averaged across all models the error in GPP is 7, 34, 34 and 13 gCm⁻²month⁻¹ for Chersky, Chokurdakh, Nur-Hakasija and Zotino, respectively. Mean errors for ER are 8, 35, 43 and 33 gCm⁻² month⁻¹, respectively.

Overall the models simulate well the seasonal cycle in GPP (Fig. 2) and ER (Fig. 3), including the timing of peak CO₂ drawdown. Modest overestimates are noted near growing season peak at Nur-Hakasija and Zotino. However, for all four sites significant over- and under- estimates in GPP and ER are also noted (Table 4). Overestimates in ER for Nur-Hakasija and Zotino during late summer and autumn are particularly noteworthy. For the two sites in the south there is a tendency for overestimation in GPP and ER. All models overestimate both GPP and ER at HAK. Overestimates of both GPP and ER are found for all models for Nur-Hakasija. Seven of the nine models overestimate GPP and ER at Zotino, with ER overestimated by a considerable degree. An ANOVA test was carried out to determine whether model errors in ER exceed the errors in GPP. The tests confirm that that ER errors are greater on average than the GPP errors for comparisons where (i) ER errors for all sites are pooled together and

Title Page

Abstract

Introduction

Conclusions

References

Tables

Figures



Back

Close

Full Screen / Esc

Printer-friendly Version

Interactive Discussion



compared against GPP pooled across all sites and (ii) ER and GPP errors for the two tundra sites are pooled and compared against ER and GPP errors for the two forest sites.

The tendency to overestimate ER leads to discrepancies in net source (negative NEP) at Nur-Hakasija and Zotino, particularly in autumn (Fig. 4). Average NEP errors are -11 and $-20 \text{ g C m}^{-2} \text{ month}^{-1}$ for Nur-Hakasija and Zotino, respectively (Table 4). For both Chersky and Chokurdakh the models simulate well both the magnitude and timing of CO_2 source activity prior to and following the dormant season. A lack of available tower-based data during the colder months limits the robustness of our assessments during that time of year.

3.1.2 Regional-level evaluation of model GPP

Estimates from the MOD17 product provide a temporally and spatially continuous benchmark to assess model simulated GPP over the study domain. Average annual-total GPP from MOD17 over the period 2000–2009 is shown in Fig. 5. The MOD17 product clearly captures three distinct landcover zones over the region, representing: (i) grasslands across the south; (ii) boreal forests in the center of the region; and (iii) tundra to the north. Highest production occurs in the western forests where mean annual temperatures are higher. Both the steppe and tundra areas show annual GPP of less than $300 \text{ g C m}^{-2} \text{ yr}^{-1}$. Areas of low productivity in high elevation areas to the north are well delineated. The spatially averaged mean across the region is approximately $470 \text{ g C m}^{-2} \text{ yr}^{-1}$. In most of the models the patterns in GPP broadly represent the major biome areas captured in the MODIS landcover product (Fig. 1a). Grid-based correlations with the MOD17 GPP estimates (upper left of map panels in Fig. 5) show a wide range of agreement across the models. Spatial averages of the correlations across the domain range from $r = 0.92$ (ISBA) to $r = 0.48$ (ORCHIDEE). Four of the nine (LPJG, MIROC, ORCHIDEE, UVic) simulate a GPP field that explains less than 44% of the variability in GPP found within the MOD17 product. Annual GPP in the LPJG is notably low across the eastern half of the region. The CLM4.5 tends to predict

BGD

12, 2257–2305, 2015

CO₂ exchange across Northern Eurasia

M. A. Rawlins et al.

Title Page

Abstract

Introduction

Conclusions

References

Tables

Figures

◀

▶

◀

▶

Back

Close

Full Screen / Esc

Printer-friendly Version

Interactive Discussion



lower GPP than MOD17 over tundra areas and higher productivity in the boreal zone. The east to west gradient is generally well simulated in most of the models. Figure 6 shows the distribution of GPP for all grids of each model. Regional averages from each model fall within $\pm 20\%$ of the MOD17 average of $468 \text{ gC m}^{-2} \text{ yr}^{-1}$, with the exception of the LPJG model for which annual GPP is 40% lower than MOD17. In general the models bracket the MOD17 estimates, with several models showing a larger spread and several showing a reduced spread.

For each model the spatial pattern in ER (not shown) closely matches the pattern in GPP, consistent with the strong dependence of autotrophic respiration and litterfall on vegetation productivity (Waring et al., 1998; Bond-Lamberty et al., 2004). Area averaged GPP and ER are highly correlated ($r = 0.99$, Fig. 7). That is, models which simulate low (high) GPP also simulate low (high) ER.

3.1.3 Spatial patterns and area averages

In this study net ecosystem productivity (NEP) represents the net exchange of CO_2 between the land surface and the atmosphere. The NEP residual CO_2 flux is defined here as the difference between GPP and ER. We did not include other emission components of land-atmosphere CO_2 exchange (Hayes and Turner, 2012) because several of the models are limited in their representation of disturbance processes important for carbon cycling in boreal forest regions (e.g. fire and forest harvest). The multimodel mean NEP is approximately $20 \text{ gC m}^{-2} \text{ yr}^{-1}$ or 270 TgC yr^{-1} over the simulation period. Among the models NEP varies from 4 (UVic) to 48 (JULES) $\text{gC m}^{-2} \text{ yr}^{-1}$, a range that is double the multimodel mean. The mean NEP is highest over the south central part of the region and lowest in the tundra to the north (Fig. 8). Only 0.3% of the region is a net annual source of CO_2 , notably two small areas in Scandinavia. Tundra areas are a net sink of approximately $15 \text{ gC m}^{-2} \text{ yr}^{-1}$ based on the multimodel mean NEP. As measured by the coefficient of variation, the agreement in NEP among the models is highest across the boreal region and lowest to the north and over the grasslands to the south.

3.2 Temporal changes over period 1960–2009

Figure 9 shows the time series of regionally averaged annual NEP each year over the period 1960–2009 for each model. Across the model group annual NEP is positive in most but not all years. Several models show a net source of CO₂ in some years, primarily during the earlier decades of the period. Among the models NEP increases by 0.01 to 0.79 gCm⁻²yr⁻², (5 to 40 gCm⁻² total over the period) based on a linear least squares (LLS) regression (Table 5). Seven of the models (CLM4.5, CoLM, ISBA, JULES, LPJG, MIROC, ORCHIDEE) show statistically significant trends at the $p < 0.01$. Taking averages over the first decade (1960–1969) and last decade (2000–2009) we estimate that the NEP change ranges from 10 to 400 % of the first decade mean, with a nine model average of 135 %. For each model the GPP trend magnitude exceeds the ER trend magnitude (Table 5), hence the increase in NEP over time. The increases from the first to last decade of the simulations range from 9–35 % of the early decade average for GPP and 8–30 % for ER. Total cumulative NEP over the 50 yr period and averaged across all models is approximately 12 (range 3–20) Pg C (Fig. 10). Averaged across the models, NEP exhibits an increase during mainly the earliest decades that tends to weaken over the latter decades (Fig. 11). The uncertainty range for the multimodel mean suggests that the region has been a net sink for CO₂ over the simulation period. Interestingly the uncertainty range reflects relatively better model agreement in annual NEP (lower variance) during the years 1960–1965 and in the low NEP years 1978 and 1996. Amid this increase there is evidence of a “deceleration” in NEP. The deceleration is apparent when examining trend magnitude and significance across all time intervals (minimum 20 yr interval) over the simulation period (Fig. 12). Here several models (ISBA, LPJG, ORCHIDEE) exhibit weaker linear trends over time and all models show a lack of significant positive trends for time intervals spanning the latter decades (e.g. 1980–1999 or 1982–2009). While temporal trends in NEP are highly variable across the models, it is clear that the greatest increases in NEP occurred during the earliest decades of the simulation period. The LLS

BGD

12, 2257–2305, 2015

CO₂ exchange across Northern Eurasia

M. A. Rawlins et al.

Title Page

Abstract

Introduction

Conclusions

References

Tables

Figures

◀

▶

◀

▶

Back

Close

Full Screen / Esc

Printer-friendly Version

Interactive Discussion



trend is significant for 20 of 42 (48 %) possible time periods beginning in 1975 or later, whereas 72 of 107 (67 %) are significant for periods starting in 1960–1962.

3.3 Residence time

Annual estimates of residence time are calculated for each model and at each grid cell over the period 1960–2009 using model soil carbon storage and the rate of heterotrophic respiration (R_h). Among the models residence time (long-term climatological mean) varies from 40 (CoLM) to 400 yr (CLM4.5), and largely by model soil carbon amount. Over the period examined all of the models simulate a statistically significant ($p < 0.01$) decrease in the regionally-averaged residence time. Across the models the decrease from first to last decade of the study period ranges from -5 to -16 % of each model's mean. The decline occurs amid an increase in SOC storage over time. All models with the exception of CoLM simulate a statistically significant increase in soil carbon and all exhibit an increase in R_h . The increases in carbon storage range from 0.2 to 3.6 % while the increases in R_h range from 7 to 22 %. Likewise the models simulate an increase in the the rate of net primary production (NPP) of 8 to 30 %. Across the model group the change in residence time is highly correlated ($r = 0.99$) with change in R_h . In essence higher rates in R_h and NPP indicate a decrease in soil carbon residence time, with increased soil carbon storage resulting from enhanced vegetation productivity and litterfall inputs.

The spatial pattern in residence time changes suggests that controlling influences are leading to both decreases and increases over different parts of the region. The largest decreases are found across north-central Russia and the eastern third of the domain (Fig. 13). The decreases in residence time are statistically significant ($p < 0.01$) for just over 46 % of the grid cells (inset, Fig. 13). The residence time decrease exceeds -20 % over approximately 16 % of the region. An increase in residence time is noted for less than 5 % of the grids, including a small area in the far north and across extreme southern parts of the region. However, the significance of those increasing trends is limited for many of the grids.

Title Page

Abstract

Introduction

Conclusions

References

Tables

Figures



Back

Close

Full Screen / Esc

Printer-friendly Version

Interactive Discussion



4 Discussion

4.1 Uncertainties in tower-based measurements

The potential for alterations to the terrestrial sink of atmospheric CO₂ across the high northern latitudes motivates our examination of model estimates of land-atmosphere exchanges of CO₂ across the arctic drainage basin of northern Eurasia. Validation of model estimates through comparisons to measured flux tower data is challenged by several factors. The limited extent of available measurements from a sparse regional tower network (only four sites and twelve site-years) makes it difficult to validate the model estimates and, in turn, identify model processes which require refinement.

There are also inherent uncertainties in GPP and ER data derived from net ecosystem exchange (NEE) measurements at the eddy covariance tower sites. ER is generally assumed to equal NEE during nighttime hours (Lasslop et al., 2010). An empirical relationship is derived to estimate ER during that time and it is extrapolated into the daylight hours. GPP is then generally calculated as the difference between NEE and ER (accounting for appropriate signs). Since there is generally daylight for photosynthesis during the middle of the summer, ER could potentially be underestimated if primary production had occurred during the hours used for ER model calibration. Direct validation of the partitioning of measured NEE flux to GPP and ER is not possible. However in a sensitivity study Lasslop et al. (2010) compared two independent methods for partitioning and found general agreement in the results. This agreement across methods increases our confidence in the partitioned GPP and ER estimates in the LaThuile FLUXNET dataset. When measurements come from nearly ideal sites the error bound on the net annual exchange of CO₂ has been estimated to be less than $\pm 50 \text{ g C m}^{-2} \text{ yr}^{-1}$ (Baldocchi, 2003). Systematic errors in eddy covariance fluxes due to non-ideal observation conditions are uncertain at this time. Total error is likely below the value of $200 \text{ g C m}^{-2} \text{ yr}^{-1}$ that has been conservatively estimated (Reichstein et al., 2007). The model errors estimated in the present study often exceed this level in the comparison for sites Nur-Hakasija and a few models do as well for Zotino.

4.2 Model uncertainties contributing to errors in net CO₂ sink/source activity

Regionally averaged GPP is within 20 % of the MOD17 average ($470 \text{ g C m}^{-2} \text{ yr}^{-1}$) for 8 of the 9 models. While the models generally capture the spatial pattern in GPP, the percentage of variance explained in several models indicates that improvements are needed. Tower-based data suggest the timing of the seasonal cycle in CO₂ drawdown and release is well captured in most of the models (Fig. 4). Yet, while peak summer drawdown and to a large extent the net CO₂ flux (NEP) is well simulated, several models overestimate by a considerable degree the net CO₂ source before and after winter dormancy. Overestimates in GPP and ER are more common than underestimates (Table 4). Indeed, all errors are positive for site Nur-Hakasija and five of the seven models show relatively large overestimates in ER at Zotino. It should be noted that large seasonal flux errors (e.g. Keenan et al., 2012; Richardson et al., 2012; Schaefer et al., 2012) will appear as more modest monthly errors such as those noted in our analysis. While it is not possible to evaluate sources of error separately for R_h and R_a , several model processes warrant investigation. The tendency to overestimate GPP suggests that model parametrization and process specifications controlling primary production may require further refinement. Other recent work supports our findings and also suggests a closer examination of model-simulated respiration rates is needed. Quegan et al. (2011) found that NPP simulated by two DGVMs examined was nearly balanced by the models' estimate of R_h . Dolman et al. (2012) find that the GPP increase from 1920 to 2008 in the DGVMs of that study is balanced equally by increases in respiration. They reported NEP over the Russian territory as an average of three methods at nearly $30 \text{ g C m}^{-2} \text{ yr}^{-1}$. The DGVM average, however, was only $4.4 \text{ g C m}^{-2} \text{ yr}^{-1}$ and so low that the authors chose to remove the estimates from their final carbon budget. This underestimate was attributed to an excess in heterotrophic respiration. Of the three models common to that study and the present one, the CLM4.5 and ORCHIDEE have among the lowest NEP magnitudes of the nine models used here (Fig. 9).

[Title Page](#)[Abstract](#)[Introduction](#)[Conclusions](#)[References](#)[Tables](#)[Figures](#)[⏪](#)[⏩](#)[◀](#)[▶](#)[Back](#)[Close](#)[Full Screen / Esc](#)[Printer-friendly Version](#)[Interactive Discussion](#)

**CO₂ exchange across
Northern Eurasia**

M. A. Rawlins et al.

Title Page

Abstract

Introduction

Conclusions

References

Tables

Figures

I◀

▶I

◀

▶

Back

Close

Full Screen / Esc

Printer-friendly Version

Interactive Discussion



Averaged across the nine models NEP is approximately $20 \text{ g C m}^{-2} \text{ yr}^{-1}$. This is more consistent with the three-method average of Dolman et al. (2012) than the lower DGVM estimates described in their study. The multimodel mean sink of $270 \text{ Tg C g C yr}^{-1}$ estimated in this study is also broadly consistent with inventory assessments for Eurasian forests which range between 93 and 347 Tg C yr^{-1} (Hayes et al., 2011). However, despite these general agreements, recent research points to phenology as one of the principle sources of error in model simulations of land–atmosphere exchanges of CO₂. Graven et al. (2013) found that the change in NEP simulated by a set of CMIP5 models could not account for the observed increase in the seasonal cycle amplitude in atmospheric CO₂ concentrations. They point to data showing that boreal regions have experienced greening and shifting age composition which strongly influence NEP and suggest that process models under-represent the observed changes. Model inability to capture canopy phenology has been identified as a major source of model uncertainty leading to large seasonal errors in carbon fluxes such as GPP (Keenan et al., 2012; Richardson et al., 2012; Schaefer et al., 2012). Indeed, evaluated against flux tower data across the Eastern US current state-of-the-art terrestrial biosphere models have been found to mis-characterize the temperature sensitivity of phenology, which contributes to poor model performance (Keenan et al., 2014). Examining 11 coupled carbon-climate models from the IPCC Fifth Assessment Report for land areas poleward of 30° N, Anav et al. (2013) found that the models consistently overestimate the mean value of leaf area index (LAI) and have an increased growing season, mostly due to a later dormancy, compared to satellite data. Several of the models also showed delayed dormancy in autumn and low spatial correlations across the pan Arctic. Delayed dormancy would explain much of the error in autumn NEP in land models that has been attributed to overestimation of R_h . Relatively low NEP simulated by several models in the present study support these findings.

Simulated R_h estimates among the DGVMs analyzed by Dolman et al. (2012) vary in the range between 200 to $225 \text{ g C m}^{-2} \text{ yr}^{-1}$. In the present study the nine model average is $190 \text{ g C m}^{-2} \text{ yr}^{-1}$. Dolman et al. (2012) point to lower estimates from Kurganova and

**CO₂ exchange across
Northern Eurasia**

M. A. Rawlins et al.

Title Page

Abstract

Introduction

Conclusions

References

Tables

Figures

I ◀

▶ I

◀

▶

Back

Close

Full Screen / Esc

Printer-friendly Version

Interactive Discussion



Nilsson (2003) of $139 \text{ g C m}^{-2} \text{ yr}^{-1}$ and Schepaschenko et al. (2013) of $174 \text{ g C m}^{-2} \text{ yr}^{-1}$ as being more representative for the region. Our benchmark comparisons of ER against tower-based data are consistent with these recent studies and suggest that several models are likely overestimating R_h , particularly over the boreal forest zone.

5 Among the model examined in this study a wide range in soil carbon parameterizations is noted (Table 2). Not surprisingly the effects of active layer depth on the availability of soil organic carbon for decomposition and combustion has been recognized as a key sensitivity in process models (Hayes et al., 2014). Regarding below-ground processes, model parameterizations and processes controlling carbon storage and turnover such as litter decomposition rates and biological activity in frozen soils (Hobbie et al., 2000)

10 require close examination as well. Model simulations of R_h during the nongrowing season are sensitive to the presence or absence of snow (McGuire et al., 2000), suggesting that future studies of mechanisms controlling winter CO₂ emissions in tundra may help resolve uncertainties in processes within land surface models and provide

15 a means to connect a warming climate with vegetation changes, permafrost thaw and CO₂ source/sink activity across high northern latitude terrestrial ecosystems.

4.3 Uncertainties in temporal trend estimates

Uncertainties exist as to whether tundra areas are presently a net sink or source of CO₂. Across tundra regions, process models indicate a stronger sink in the 2000s compared with the 1990s, attributable to a greater increase in vegetation net primary production than heterotrophic respiration in response to warming (McGuire et al., 2012; Belshe et al., 2013). The spatial pattern in multimodel mean NEP in this study points to small areas in Scandinavia (< 1 % of the domain) as sources of CO₂. Broadly, areas classified as tundra are a modest CO₂ sink of approximately $15 \text{ g C m}^{-2} \text{ yr}^{-1}$. Estimates

20 of NEP sink magnitudes must be interpreted with caution knowing that the models in general possess inadequate representation of disturbances which are an important component of the overall carbon balance (Hayes et al., 2011). Only two of the models

25

analyzed here include a dynamic vegetation component. The absence of time-varying vegetation specifications also limits our ability to more accurately assess the influence of changing species composition on NEP in tundra areas. Models must also take into account lateral carbon fluxes and methane (CH₄) in order to characterize a more comprehensive carbon budget.

Previous studies have pointed to changes in the seasonal drawdown and release of CO₂ across the northern high latitudes (Graven et al., 2013). A change in the seasonal cycle of GPP and ER is also noted (figure not shown), with the models analyzed in this study simulating a relatively higher productivity rate from late spring to mid-summer. Indeed, increased productivity did not occur uniformly across the growing season, as most of the models show little change in August or September NEP over time. The models also simulate little change in NEP over the cold season. Greater productivity in spring and early summer may be due in part to earlier spring thawing and temporal advance in growing season initiation (McDonald et al., 2004), whereas GPP and NEP are more strongly constrained by moisture limitations later in the growing season (Yi et al., 2014). Extension of the growing season is therefore attributed more to a regional warming driven advance in spring thaw than a delay in autumn freeze-up (Kimball et al., 2006; Euskirchen et al., 2006; Kim et al., 2012) which correlates with regional annual evapotranspiration for the region above 40° N (Zhang et al., 2011). There are however signs of a delay in the timing of the fall freeze (-5.4 days decade⁻¹) across Eurasia over the period 1988–2002 (Smith et al., 2004) consistent with fall satellite snow cover (SCE) increases, and attributed to greater fall/winter snowfall and regional cooling (Cohen et al., 2012). Consistent with the advance in spring thaw, the models examined here show a greater NEP increase in spring compared to autumn.

Soil carbon storage across the region increased significantly over the study period in eight of the nine models. A relatively larger increase in R_h is correlated strongly with the associated decline in soil carbon residence time. This suggests that amid recent warming, vegetation carbon inputs to the soil were greater than the enhancement in decomposition. In a recent study involving CMIP5 models, Carvalhais et al. (2014)

BGD

12, 2257–2305, 2015

CO₂ exchange across Northern Eurasia

M. A. Rawlins et al.

Title Page

Abstract

Introduction

Conclusions

References

Tables

Figures

◀

▶

◀

▶

Back

Close

Full Screen / Esc

Printer-friendly Version

Interactive Discussion



**CO₂ exchange across
Northern Eurasia**

M. A. Rawlins et al.

Title Page

Abstract

Introduction

Conclusions

References

Tables

Figures

I◀

▶I

◀

▶

Back

Close

Full Screen / Esc

Printer-friendly Version

Interactive Discussion



found that while the coupled climate/carbon-cycle models reproduce the latitudinal patterns of carbon turnover times, differences between the models of more than one order of magnitude were also noted. The authors suggest that more accurate descriptions of hydrological processes and water–carbon interactions are needed to improve the model estimates of ecosystem carbon turnover times. Apart from climatological factors, vegetation growth is also dependent on biological nitrogen availability. Failure to account for nitrogen limitation may thus impart a bias in the modeled carbon flux estimates. However, more process models are incorporating linkages between carbon and nitrogen dynamics (Thornton et al., 2009). Given the broad range in spatial patterns in GPP across the models, a closer examination of processes related to nitrogen limitations and primary production is needed. The lower rate of NEP increase over the latter decades of the simulation period suggests a weakening of the land CO₂ sink, driven by increased R_h from warming, associated permafrost thaw, and an upward trend in fire emissions (Hayes et al., 2011).

5 Conclusions

Outputs from a suite of land surface models were used to investigate elements of the land–atmosphere exchange of CO₂ across northern Eurasia over the period 1960–2009. Evaluated against tower data, overestimates in both GPP and ER are noted in several of the models, with larger errors in ER relative to GPP, particularly for the comparisons at the two forest sites. Regarding agreement in the spatial pattern in GPP, less than half of the variance in GPP expressed in the MOD17 product is explained by the GPP pattern from four of the nine models. Over the simulation period NEP increases between 10 and 400 % of the respective model mean. The models exhibit a decrease in residence time of the soil carbon pool that is driven by an increase in R_h , simultaneous with an increase in soil carbon storage. This suggests that net primary productivity (NPP) inputs to the pool increased more than R_h fluxes out.

**CO₂ exchange across
Northern Eurasia**

M. A. Rawlins et al.

[Title Page](#)[Abstract](#)[Introduction](#)[Conclusions](#)[References](#)[Tables](#)[Figures](#)[I ◀](#)[▶ I](#)[◀](#)[▶](#)[Back](#)[Close](#)[Full Screen / Esc](#)[Printer-friendly Version](#)[Interactive Discussion](#)

Several recommendations are made as a result of this analysis. The range in area and climatological mean NEP across the models, more than double the mean value, illustrates the considerable uncertainty in the magnitude of the contemporary CO₂ sink. The results of the site-level comparison point to a need to better understand the connections between model simulated productivity rates, soil dynamics controlling heterotrophic respiration rates, and errors in total ER. Given the strong connections between soil thermal and hydrological variations and soil respiration, we recommend that model improvements are targeted at processes and parameterizations controlling soil respiration with depth in the soil profile. These validation efforts are especially important given the likelihood of net carbon transfer from ecosystems to the atmosphere from permafrost thaw (Schuur and Abbott, 2012). Model responses to CO₂ fertilization and nitrogen limitation, processes largely underrepresented in the models, should be evaluated in the context of ecosystem productivity in this region. While insights have been gained by examining the model estimates of GPP, ER, and NEP, an improved understanding of the net CO₂ sink/source activity will require improvements in carbon losses due to fire and other disturbances. The limited number of measured site data across this important region clearly hampers model assessments, highlighting the critical need for new field, tower, and aircraft data for model validation and parametrization. Specifically, new observations in the boreal zone are needed to further evaluate model biases documented in this and in other recent studies. Moreover, our finding of elevated CO₂ source activity during the shoulder seasons points to a critical need for more observations during autumn, winter, and spring. New observations from current and upcoming field campaigns such as Carbon in Arctic Reservoirs Vulnerability Experiment (CARVE) and the Arctic Boreal Vulnerability Experiment (ABoVE) should be used to confirm our results. Future model evaluations will benefit from continued development of consistent benchmarking datasets from field measurements and remote sensing. Regarding tower data, any new measurements must be supported by refinements in the models used to partition the measured NEE flux into GPP and ER components. Regarding these and similar model intercomparisons, investments must be made which will min-

imize or eliminate differences in a priori climate forcings used in the simulations. At a programmatic level support for these activities should lead to well designed model intercomparisons which minimize, to the extent possible, differences in model forcings and other elements which confound model intercomparisons.

5 *Author contributions.* M. A. Rawlins conceived the study with input from A. D. McGuire, J. K. Kimball and P. Dass. Co-authors D. Lawrence, E. Burke, X. Chen, C. Delire, C. Koven, A. MacDougall, S. Peng, A. Rinke, K. Saito, W. Zhang, R. Alkama, T. J. Bohn, P. Ciais, B. Decharme, I. Gouttevin, T. Hajima, D. Ji, G. Krinner, D. P. Lettenmaier, P. Miller, J. C. Moore, B. Smith, and T. Sueyoshi provided model simulation outputs. M. A. Rawlins analyzed the
10 outputs and other data. M. A. Rawlins prepared the manuscript with contributions from all co-authors.

Acknowledgements. This research was supported by the U.S. National Aeronautics and Space Administration NASA grant NNX11AR16G and the Permafrost Carbon Network (<http://www.permafrostcarbon.org/>) funded by the National Science Foundation. The MODIS Land Cover
15 Type product data was obtained through the online Data Pool at the NASA Land Processes Distributed Active Archive Center (LP DAAC), USGS/Earth Resources Observation and Science (EROS) Center, Sioux Falls, South Dakota (https://lpdaac.usgs.gov/data_access). We thank the researchers working at FLUXNET sites for kindly providing CO₂ flux data. We also thank Eugenie Euskirchen and Dan Hayes for comments on an earlier version of the manuscript, and Yonghong Yi for assistance with the FLUXNET data. Charles Koven was supported by
20 the Director of the Office of Biological and Environmental Research, Office of Science, U.S. Department of Energy, under Contract DE-AC02-05CH11231 as part of the Regional and Global Climate Modeling Program (RGCM). Eleanor J. Burke was supported by the Joint UK DECC/Defra Met Office Hadley Centre Climate Programme (GA01101) and the European Union Seventh Framework Programme (FP7/2007–2013) under grant agreement no. 282700. Several of the coauthors were funded by the European Union 7th Framework Programme under project Page21 (grant 282700). Any use of trade, firm, or product names is for descriptive purposes only and does not imply endorsement by the U.S. Government.

BGD

12, 2257–2305, 2015

CO₂ exchange across Northern Eurasia

M. A. Rawlins et al.

Title Page

Abstract

Introduction

Conclusions

References

Tables

Figures

◀

▶

◀

▶

Back

Close

Full Screen / Esc

Printer-friendly Version

Interactive Discussion



References

- Anav, A., Murray-Tortarolo, G., Friedlingstein, P., Sitch, S., Piao, S., and Zhu, Z.: Evaluation of land surface models in reproducing satellite Derived leaf area index over the high-latitude Northern Hemisphere. Part II: Earth system models, *Remote Sens.*, 5, 3637–3661, 2013. 2273
- Avis, C. A., Weaver, A. J., and Meissner, K. J.: Reduction in areal extent of high-latitude wetlands in response to permafrost thaw, *Nat. Geosci.*, 4, 444–448, 2011. 2263
- Baldocchi, D.: Turner Review No. 15. “Breathing” of the terrestrial biosphere: lessons learned from a global network of carbon dioxide flux measurement systems, *Aust. J. Bot.*, 56, 1–26, 2008. 2264, 2290, 2291
- Baldocchi, D. D.: Assessing the eddy covariance technique for evaluating carbon dioxide exchange rates of ecosystems: past, present and future, *Glob. Change Biol.*, 9, 479–492, 2003. 2271
- Belshe, E., Schuur, E., and Bolker, B.: Tundra ecosystems observed to be CO₂ sources due to differential amplification of the carbon cycle, *Ecol. Lett.*, 16, 1307–1315, 2013. 2261, 2274
- Best, M. J., Pryor, M., Clark, D. B., Rooney, G. G., Essery, R. L. H., Ménard, C. B., Edwards, J. M., Hendry, M. A., Porson, A., Gedney, N., Mercado, L. M., Sitch, S., Blyth, E., Boucher, O., Cox, P. M., Grimmond, C. S. B., and Harding, R. J.: The Joint UK Land Environment Simulator (JULES), model description – Part 1: Energy and water fluxes, *Geosci. Model Dev.*, 4, 677–699, doi:10.5194/gmd-4-677-2011, 2011. 2263
- Bohn, T. J., Podest, E., Schroeder, R., Pinto, N., McDonald, K. C., Glagolev, M., Filippov, I., Maksyutov, S., Heimann, M., Chen, X., and Lettenmaier, D. P.: Modeling the large-scale effects of surface moisture heterogeneity on wetland carbon fluxes in the West Siberian Lowland, *Biogeosciences*, 10, 6559–6576, doi:10.5194/bg-10-6559-2013, 2013. 2263
- Bond-Lamberty, B., Wang, C., and Gower, S. T.: A global relationship between the heterotrophic and autotrophic components of soil respiration?, *Glob. Change Biol.*, 10, 1756–1766, 2004. 2268
- Carvalhais, N., Forkel, M., Khomik, M., Bellarby, J., Jung, M., Migliavacca, M., Mu, M., Saatchi, S., Santoro, M., Thurner, M., Weber, U., Ahrens, B., Beer, C., Cescatti, A., Randerson, J. T., and Reichstein, M.: Global covariation of carbon turnover times with climate in terrestrial ecosystems, *Nature*, 514, 213–217, doi:10.1038/nature13731, 2014. 2275

BGD

12, 2257–2305, 2015

CO₂ exchange across Northern Eurasia

M. A. Rawlins et al.

Title Page

Abstract

Introduction

Conclusions

References

Tables

Figures

◀

▶

◀

▶

Back

Close

Full Screen / Esc

Printer-friendly Version

Interactive Discussion



**CO₂ exchange across
Northern Eurasia**

M. A. Rawlins et al.

Title Page

Abstract

Introduction

Conclusions

References

Tables

Figures

I◀

▶I

◀

▶

Back

Close

Full Screen / Esc

Printer-friendly Version

Interactive Discussion



- Chapin III, F. S., Sturm, M., Serreze, M. C., McFadden, J. P., Key, J. R., Lloyd, A. H.,
McGuire, A. D., Rupp, T. S., Lynch, A. H., Schimel, J. P., Beringer, J., Chapman, W. L.,
Epstein, H. E., Euskirchen, E. S., Hinzman, L. D., Jia, G., Ping, C.-L., Tape, K. D., Thomp-
son, C. D. C., Walker, D. A., and Welker, J. M.: Role of land-surface changes in Arctic summer
warming, *Science*, 310, 657–660, doi:10.1126/science.1117368, 2005. 2263
- Clark, D. B., Mercado, L. M., Sitch, S., Jones, C. D., Gedney, N., Best, M. J., Pryor, M.,
Rooney, G. G., Essery, R. L. H., Blyth, E., Boucher, O., Harding, R. J., Huntingford, C., and
Cox, P. M.: The Joint UK Land Environment Simulator (JULES), model description – Part 2:
Carbon fluxes and vegetation dynamics, *Geosci. Model Dev.*, 4, 701–722, doi:10.5194/gmd-
4-701-2011, 2011. 2263
- Cohen, J. L., Furtado, J. C., Barlow, M. A., Alexeev, V. A., and Cherry, J. E.: Arctic warming,
increasing snow cover and widespread boreal winter cooling, *Environ. Res. Lett.*, 7, 501–
506, 2012. 2275
- Cox, P. M., Betts, R. A., Jones, C. D., Spall, S. A., and Totterdell, I. J.: Acceleration of global
warming due to carbon-cycle feedbacks in a coupled climate model, *Nature*, 408, 184–187,
doi:10.1038/35041539, 2000. 2260
- Crutzen, P. J.: The “Anthropocene”, in: *Earth System Science in the Anthropocene*, edited
by: Ehlers, P. D. E. and Krafft, D. T., Springer, Berlin, Heidelberg, 13–18, available at: http://link.springer.com/chapter/10.1007/3-540-26590-2_3, 2006. 2260
- Dai, Y., Zeng, X., Dickinson, R. E., Baker, I., Bonan, G. B., Bosilovich, M. G., Denning, A. S.,
Dirmeyer, P. A., Houser, P. R., Niu, G., et al.: The common land model, *B. Am. Meteorol.
Soc.*, 84, doi:10.012/201590876, 2003. 2263
- Dai, Y., Dickinson, R. E., and Wang, Y.-P.: A two-big-leaf model for canopy temperature, photo-
synthesis, and stomatal conductance., *J. Climate*, 17, 2281–2299, 2004. 2263
- Decharme, B., Boone, A., Delire, C., and Noilhan, J.: Local evaluation of the interaction between
soil biosphere atmosphere soil multilayer diffusion scheme using four pedotransfer functions,
J. Geophys. Res.-Atmos., 116, D20126, doi:10.1029/2011JD01600.2, 2011. 2263
- Dolman, A. J., Shvidenko, A., Schepaschenko, D., Ciais, P., Tchebakova, N., Chen, T.,
van der Molen, M. K., Belelli Marchesini, L., Maximov, T. C., Maksyutov, S., and Schulze, E.-
D.: An estimate of the terrestrial carbon budget of Russia using inventory-based, eddy covari-
ance and inversion methods, *Biogeosciences*, 9, 5323–5340, doi:10.5194/bg-9-5323-2012,
2012. 2261, 2264, 2272, 2273

CO₂ exchange across
Northern Eurasia

M. A. Rawlins et al.

Title Page

Abstract

Introduction

Conclusions

References

Tables

Figures

◀

▶

◀

▶

Back

Close

Full Screen / Esc

Printer-friendly Version

Interactive Discussion



- Dutta, K., Schuur, E. A. G., Neff, J. C., and Zimov, S. A.: Potential carbon release from permafrost soils of Northeastern Siberia, *Glob. Change Biol.*, 12, 2336–2351, doi:10.1111/j.1365-2486.2006.01259.x, 2006. 2260
- Euskirchen, E., McGuire, A. D., Kicklighter, D. W., Zhuang, Q., Clein, J. S., Dargaville, R., Dye, D., Kimball, J. S., McDonald, K. C., Melillo, J. M., et al.: Importance of recent shifts in soil thermal dynamics on growing season length, productivity, and carbon sequestration in terrestrial high-latitude ecosystems, *Glob. Change Biol.*, 12, 731–750, 2006. 2260, 2275
- Fisher, J. B., Sikka, M., Oechel, W. C., Huntzinger, D. N., Melton, J. R., Koven, C. D., Ahlström, A., Arain, M. A., Baker, I., Chen, J. M., Ciais, P., Davidson, C., Dietze, M., El-Masri, B., Hayes, D., Huntingford, C., Jain, A. K., Levy, P. E., Lomas, M. R., Poulter, B., Price, D., Sahoo, A. K., Schaefer, K., Tian, H., Tomelleri, E., Verbeeck, H., Viogy, N., Wania, R., Zeng, N., and Miller, C. E.: Carbon cycle uncertainty in the Alaskan Arctic, *Biogeosciences*, 11, 4271–4288, doi:10.5194/bg-11-4271-2014, 2014. 2261
- Goetz, S. J., Bunn, A. G., Fiske, G. J., and Houghton, R.: Satellite-observed photosynthetic trends across boreal North America associated with climate and fire disturbance, *P. Natl. Acad. Sci. USA*, 102, 13521–13525, 2005. 2260
- Goetz, S. J., Fiske, G. J., and Bunn, A. G.: Using satellite time-series data sets to analyze fire disturbance and forest recovery across Canada, *Remote Sens. Environ.*, 101, 352–365, 2006. 2260
- Gouttevin, I., Menegoz, M., Dominé, F., Krinner, G., Koven, C., Ciais, P., Tarnocai, C., and Boike, J.: How the insulating properties of snow affect soil carbon distribution in the continental pan-Arctic area, *J. Geophys. Res.-Biogeo.*, 117, G02020, doi:10.1029/2011JG001916, 2012. 2263
- Graven, H., Keeling, R., Piper, S., Patra, P., Stephens, B., Wofsy, S., Welp, L., Sweeney, C., Tans, P., Kelley, J., et al.: Enhanced seasonal exchange of CO₂ by northern ecosystems since 1960, *Science*, 341, 1085–1089, 2013. 2260, 2273, 2275
- Groisman, P. and Soja, A. J.: Ongoing climatic change in Northern Eurasia: justification for expedient research, *Environ. Res. Lett.*, 4, 045002, doi:10.1088/1748-9326/4/4/045002, 2009. 2262
- Groisman, P. Y. and Bartalev, S. A.: Northern Eurasia Earth Science Partnership Initiative (NEESPI), science plan overview, *Global Planet. Change*, 56, 215–234, 2007. 2262
- Groisman, P. Y., Clark, E. A., Lettenmaier, D. P., Kattsov, V. M., Sokolik, I. N., Aizen, V. B., Cartus, O., Chen, J., Schmullius, C. C., Conard, S., et al.: The Northern Eurasia earth science

**CO₂ exchange across
Northern Eurasia**

M. A. Rawlins et al.

[Title Page](#)[Abstract](#)[Introduction](#)[Conclusions](#)[References](#)[Tables](#)[Figures](#)[I◀](#)[▶I](#)[◀](#)[▶](#)[Back](#)[Close](#)[Full Screen / Esc](#)[Printer-friendly Version](#)[Interactive Discussion](#)

partnership: an example of science applied to societal needs, *B. Am. Meteorol. Soc.*, 90, 671–688, 2009. 2262

Hayes, D. and Turner, D.: The need for “apples-to-apples” comparisons of carbon dioxide source and sink estimates, *EOS T. Am. Geophys. Un.*, 93, 404–405, 2012. 2268

5 Hayes, D. J., McGuire, A. D., Kicklighter, D. W., Gurney, K., Burnside, T., and Melillo, J. M.: Is the northern high-latitude land-based CO₂ sink weakening?, *Global Biogeochem. Cy.*, 25, GB3018, doi:10.1029/2010GB003813, 2011. 2261, 2273, 2274, 2276

10 Hayes, D. J., Kicklighter, D. W., McGuire, A. D., Chen, M., Zhuang, Q., Yuan, F., Melillo, J. M., and Wullschleger, S. D.: The impacts of recent permafrost thaw on land–atmosphere greenhouse gas exchange, *Environ. Res. Lett.*, 9, 045005, doi:10.1088/1748-9326/9/4/045005, 2014. 2274

Hobbie, S. E., Schimel, J. P., Trumbore, S. E., and Randerson, J. R.: Controls over carbon storage and turnover in high-latitude soils, *Glob. Change Biol.*, 6, 196–210, doi:10.1046/j.1365-2486.2000.06021.x, 2000. 2274

15 International Permafrost Association Standing Committee on Data Information and Communication (comp.): Circumpolar Active-Layer Permafrost System (CAPS), Tech. rep., National Snow and Ice Data Center, doi:10.7265/N5SF2T3B, 2003.

20 Keenan, T., Baker, I., Barr, A., Ciais, P., Davis, K., Dietze, M., Dragoni, D., Gough, C. M., Grant, R., Hollinger, D., et al.: Terrestrial biosphere model performance for inter-annual variability of land–atmosphere CO₂ exchange, *Glob. Change Biol.*, 18, 1971–1987, 2012. 2272, 2273

25 Keenan, T. F., Gray, J., Friedl, M. A., Toomey, M., Bohrer, G., Hollinger, D. Y., Munger, J. W., O’Keefe, J., Schmid, H. P., Wing, I. S., et al.: Net carbon uptake has increased through warming-induced changes in temperate forest phenology, *Nat. Clim. Change*, 4991, 324–327, 2014. 2273

Kim, Y., Kimball, J., Zhang, K., and McDonald, K.: Satellite detection of increasing Northern Hemisphere non-frozen seasons from 1979 to 2008: Implications for regional vegetation growth, *Remote Sens. Environ.*, 121, 472–487, 2012. 2275

30 Kimball, J., McDonald, K., and Zhao, M.: Spring thaw and its effect on terrestrial vegetation productivity in the western Arctic observed from satellite microwave and optical remote sensing, *Earth Interact.*, 10, 1–22, 2006. 2275

Koven, C., Friedlingstein, P., Ciais, P., Khvorostyanov, D., Krinner, G., and Tarnocai, C.: On the formation of high-latitude soil carbon stocks: effects of cryoturbation and insu-

**CO₂ exchange across
Northern Eurasia**

M. A. Rawlins et al.

[Title Page](#)[Abstract](#)[Introduction](#)[Conclusions](#)[References](#)[Tables](#)[Figures](#)[I◀](#)[▶I](#)[◀](#)[▶](#)[Back](#)[Close](#)[Full Screen / Esc](#)[Printer-friendly Version](#)[Interactive Discussion](#)

lation by organic matter in a land surface model, *Geophys. Res. Lett.*, 36, L21501, doi:10.1029/2009GL040150, 2009. 2263

Koven, C. D., Ringeval, B., Friedlingstein, P., Ciais, P., Cadule, P., Khvorostyanov, D., Krinner, G., and Tarnocai, C.: Permafrost carbon-climate feedbacks accelerate global warming, *P. Natl. Acad. Sci. USA*, 108, 14769–14774, 2011. 2261, 2263

Kurganova, I. and Nilsson, S.: Carbon dioxide emission from soils of Russian terrestrial ecosystems, Interim Report, IR-02, 70, 2003. 2273

Lasslop, G., Reichstein, M., Papale, D., Richardson, A. D., Arneeth, A., Barr, A., Stoy, P., and Wohlfahrt, G.: Separation of net ecosystem exchange into assimilation and respiration using a light response curve approach: critical issues and global evaluation, *Glob. Change Biol.*, 16, 187–208, 2010. 2271

MacDougall, A. H., Eby, M., and Weaver, A. J.: If anthropogenic CO₂ emissions cease, will atmospheric CO₂ concentration continue to increase?, *J. Climate*, 26, 9563–9576, 2013. 2261, 2263

McDonald, K. C., Kimball, J. S., Njoku, E., Zimmermann, R., and Zhao, M.: Variability in spring-time thaw in the terrestrial high latitudes: monitoring a major control on biospheric assimilation of atmospheric CO₂ with spaceborne microwave remote sensing, *Earth Interact.*, 8, 1–23, 2004. 2275

McGuire, A., Melillo, J., Randerson, J., Parton, W., Heimann, M., Meier, R., Clein, J., Kicklighter, D., and Sauf, W.: Modeling the effects of snowpack on heterotrophic respiration across northern temperate and high latitude regions: comparison with measurements of atmospheric carbon dioxide in high latitudes, *Biogeochemistry*, 48, 91–114, doi:10.1023/A:1006286804351, 2000. 2274

McGuire, A. D., Christensen, T. R., Hayes, D., Heroult, A., Euskirchen, E., Kimball, J. S., Koven, C., Lafleur, P., Miller, P. A., Oechel, W., Peylin, P., Williams, M., and Yi, Y.: An assessment of the carbon balance of Arctic tundra: comparisons among observations, process models, and atmospheric inversions, *Biogeosciences*, 9, 3185–3204, doi:10.5194/bg-9-3185-2012, 2012. 2260, 2264, 2274

Melillo, J. M., McGuire, A. D., Kicklighter, D. W., Moore, B., Vorosmarty, C. J., and Schloss, A. L.: Global climate change and terrestrial net primary production, *Nature*, 363, 234–240, 1993. 2260

Miller, P. A. and Smith, B.: Modelling tundra vegetation response to recent arctic warming, *Ambio*, 41, 281–291, 2012. 2263

CO₂ exchange across Northern Eurasia

M. A. Rawlins et al.

Title Page

Abstract

Introduction

Conclusions

References

Tables

Figures



Back

Close

Full Screen / Esc

Printer-friendly Version

Interactive Discussion



Myneni, R. B., Keeling, C. D., Tucker, C. J., Asrar, G., and Nemani, R. R.: Increased plant growth in the northern high latitudes from 1981 to 1991, *Nature*, 386, 698–702, doi:10.1038/386698a0, 1997. 2260

Oak Ridge National Laboratory: MODIS (MCD12Q1) Land Cover Product, available at: <https://lpdaac.usgs.gov>, Land Processes Distributed Active Archive Center (LP DAAC), Sioux Falls, South Dakota, USA (last access: 1 July 2014), 2014.

Oechel, W. C., Laskowski, C. A., Burba, G., Gioli, B., and Kalthori, A. A. M.: Annual patterns and budget of CO₂ flux in an Arctic tussock tundra ecosystem, *J. Geophys. Res.-Biogeo.*, 119, 323–339, doi:10.1002/2013JG002431, 2014. 2261

Oleson, K., Lawrence, D., Bonan, G., Drewniak, B., Huang, M., Koven, C., Levis, S., Li, F., Riley, W., Subin, Z., Swenson, S., Thornton, P., Bozbiyik, A., Fisher, R., Kluzek, E., Lamarque, J., Lawrence, P., Leung, L., Lipscomb, W., Muszala, S., Ricciuto, D., Sacks, W., Sun, Y., Tang, J., and Yang, Z.: Technical Description of Version 4.5 of the Community Land Model (CLM), Ncar Technical Note NCAR/TN-503+STR, Tech. rep., National Center for Atmospheric Research, Boulder, CO, doi:10.5065/D6RR1W7M, 422 pp., 2013. 2263

Piao, S., Sitch, S., Ciais, P., Friedlingstein, P., Peylin, P., Wang, X., Ahlström, A., Anav, A., Canadell, J. G., Cong, N., et al.: Evaluation of terrestrial carbon cycle models for their response to climate variability and to CO₂ trends, *Glob. Change Biol.*, 19, 2117–2132, 2013. 2264

Pries, C. E. H., Schuur, E. A. G., and Crummer, K. G.: Holocene carbon stocks and carbon accumulation rates altered in soils undergoing permafrost thaw, *Ecosystems*, 15, 162–173, doi:10.1007/s10021-011-9500-4, 2012. 2260

Quegan, S., Beer, C., Shvidenko, A., McCallum, I., Handoh, I. C., Peylin, P., Roedenbeck, C., Lucht, W., Nilsson, S., and Schimmlus, C.: Estimating the carbon balance of central Siberia using a landscape-ecosystem approach, atmospheric inversion and Dynamic Global Vegetation Models, *Glob. Change Biol.*, 17, 351–365, 2011. 2261, 2272

Reichstein, M., Falge, E., Baldocchi, D., Papale, D., Aubinet, M., Berbigier, P., Bernhofer, C., Buchmann, N., Gilmanov, T., Granier, A., et al.: On the separation of net ecosystem exchange into assimilation and ecosystem respiration: review and improved algorithm, *Glob. Change Biol.*, 11, 1424–1439, 2005. 2265, 2290

Reichstein, M., Papale, D., Valentini, R., Aubinet, M., Bernhofer, C., Knohl, A., Laurila, T., Lindroth, A., Moors, E., Pilegaard, K., et al.: Determinants of terrestrial ecosystem carbon bal-

CO₂ exchange across
Northern Eurasia

M. A. Rawlins et al.

Title Page

Abstract

Introduction

Conclusions

References

Tables

Figures

I ◀

▶ I

◀

▶

Back

Close

Full Screen / Esc

Printer-friendly Version

Interactive Discussion



ance inferred from European eddy covariance flux sites, *Geophys. Res. Lett.*, 34, L01402, doi:10.1029/2006GL027880, 2007. 2271

Richardson, A. D., Anderson, R. S., Arain, M. A., Barr, A. G., Bohrer, G., Chen, G., Chen, J. M., Ciais, P., Davis, K. J., Desai, A. R., et al.: Terrestrial biosphere models need better representation of vegetation phenology: results from the North American Carbon Program Site Synthesis, *Glob. Change Biol.*, 18, 566–584, 2012. 2272, 2273

Rinke, A., Wang, W., Moore, J. C., Ji, D., Cui, X., Peng, S., Lawrence, D. M., McGuire, A. D., Burke, E. J., Chen, X., Delire, C., Koven, C., MacDougall, A., Saito, K., Zhang, W., Alkama, R., Bohn, T. J., Ciais, P., Decharme, B., Gouttevin, I., Hajima, T., Krinner, G., Lettenmaier, D. P., Miller, P., Smith, B., and Sueyoshi, T.: Evaluation of air-soil temperature relationships simulated by land surface models during winter across the permafrost region, *J. Geophys. Res.-Atmos.*, in review, 2014. 2264

Running, S., Nemani, R., Heinsch, F., Zhao, M., Reeves, M., and Hashimoto, H.: A continuous satellite-derived measure of global terrestrial primary production, *Bioscience*, 54, 547–560, 2004. 2265

Schaefer, K., Zhang, T., Bruhwiler, L., and Barrett, A.: Amount and timing of permafrost carbon release in response to climate warming, *Tellus B*, 63, 165–180, 2011. 2261

Schaefer, K., Schwalm, C. R., Williams, C., Arain, M. A., Barr, A., Chen, J. M., Davis, K. J., Dimitrov, D., Hilton, T. W., Hollinger, D. Y., et al.: A model-data comparison of gross primary productivity: results from the North American Carbon Program site synthesis, *J. Geophys. Res.-Biogeo.*, 117, G03010, doi:10.1029/2012JG001960, 2012. 2272, 2273

Schepaschenko, D., Mukhortova, L., Shvidenko, A., and Vedrova, E.: The pool of organic carbon in the soils of Russia, *Eurasian Soil Sci.*, 46, 107–116, 2013. 2274

Schuur, E., Vogel, J. G., Crummer, K. G., Lee, H., Sickman, J. O., and Osterkamp, T. E.: The effect of permafrost thaw on old carbon release and net carbon exchange from tundra, *Nature*, 459, 556–559, 2009. 2260

Schuur, E. A. G. and Abbott, B.: Climate change: high risk of permafrost thaw, *Nature*, 480, 32–33, doi:10.1038/480032a, 2011. 2277

Serreze, M. C. and Barry, R. G.: Processes and impacts of Arctic amplification: a research synthesis, *Global Planet. Change*, 77, 85–96, 2011. 2260

Smith, B., Prentice, I. C., and Sykes, M. T.: Representation of vegetation dynamics in the modelling of terrestrial ecosystems: comparing two contrasting approaches within European climate space, *Global Ecol. Biogeogr.*, 10, 621–637, 2001. 2263

CO₂ exchange across
Northern Eurasia

M. A. Rawlins et al.

Title Page

Abstract

Introduction

Conclusions

References

Tables

Figures

I◀

▶I

◀

▶

Back

Close

Full Screen / Esc

Printer-friendly Version

Interactive Discussion



- Smith, N. V., Saatchi, S. S., and Randerson, J. T.: Trends in high northern latitude soil freeze and thaw cycles from 1988 to 2002, *J. Geophys. Res.-Atmos.*, 109, D12101, doi:10.1029/2003JD004472, 2004. 2275
- Thornton, P. E., Doney, S. C., Lindsay, K., Moore, J. K., Mahowald, N., Randerson, J. T.,
5 Fung, I., Lamarque, J.-F., Feddes, J. J., and Lee, Y.-H.: Carbon-nitrogen interactions regulate climate-carbon cycle feedbacks: results from an atmosphere-ocean general circulation model, *Biogeosciences*, 6, 2099–2120, doi:10.5194/bg-6-2099-2009, 2009. 2276
- Vogel, J., Schuur, E. A. G., Trucco, C., and Lee, H.: Response of CO₂ exchange in a tussock tundra ecosystem to permafrost thaw and thermokarst development, *J. Geophys. Res.-Biogeo.*,
10 114, G04018, doi:10.1029/2008JG000901, 2009. 2260
- Wania, R., Ross, I., and Prentice, I.: Integrating peatlands and permafrost into a dynamic global vegetation model: 1. Evaluation and sensitivity of physical land surface processes, *Global Biogeochem. Cy.*, 23, GB3014, doi:10.1029/2008GB003412, 2009a. 2263
- Wania, R., Ross, I., and Prentice, I.: Integrating peatlands and permafrost into a dynamic global
15 vegetation model: 2. Evaluation and sensitivity of vegetation and carbon cycle processes, *Global Biogeochem. Cy.*, 23, GB3015, doi:10.1029/2008GB003413, 2009b. 2263
- Wania, R., Ross, I., and Prentice, I. C.: Implementation and evaluation of a new methane model within a dynamic global vegetation model: LPJ-WHyMe v1.3.1, *Geosci. Model Dev.*, 3, 565–584, doi:10.5194/gmd-3-565-2010, 2010. 2263
- 20 Waring, R., Landsberg, J., and Williams, M.: Net primary production of forests: a constant fraction of gross primary production?, *Tree Physiol.*, 18, 129–134, 1998. 2268
- Watanabe, S., Hajima, T., Sudo, K., Nagashima, T., Takemura, T., Okajima, H., Nozawa, T., Kawase, H., Abe, M., Yokohata, T., Ise, T., Sato, H., Kato, E., Takata, K., Emori, S., and Kawamiya, M.: MIROC-ESM 2010: model description and basic results of CMIP5-20c3m
25 experiments, *Geosci. Model Dev.*, 4, 845–872, doi:10.5194/gmd-4-845-2011, 2011. 2263
- Yi, Y., Kimball, J. S., and Reichle, R. H.: Spring hydrology determines summer net carbon uptake in northern ecosystems, *Environ. Res. Lett.*, 9, 064003, doi:10.1088/1748-9326/9/6/064003, 2014. 2275
- Zhang, K., Kimball, J. S., Hogg, E. H., Zhao, M., Oechel, W. C., Cassano, J. J.,
30 and Running, S. W.: Satellite-based model detection of recent climate-driven changes in northern high-latitude vegetation productivity, *J. Geophys. Res.*, 113, g03033, doi:10.1029/2007JG000621, 2008. 2260

Zhang, K., Kimball, J. S., Kim, Y. and McDonald, K. C.: Changing freeze-thaw seasons in northern high latitudes and associated influences on evapotranspiration, *Hydrol. Process.*, 25, 4142–4151, 2011. 2275

5 Zhao, M. and Running, S. W.: Drought-induced reduction in global terrestrial net primary production from 2000 through 2009, *Science*, 329, 940–943, 2010. 2265

Zhao, M., Heisch, F. A., Nemani, R. R., and Running, S. W.: Improvements of the MODIS terrestrial gross and net primary production global data set, *Remote Sens. Environ.*, 95, 164–176, 2005. 2265

BGD

12, 2257–2305, 2015

CO₂ exchange across Northern Eurasia

M. A. Rawlins et al.

Title Page

Abstract

Introduction

Conclusions

References

Tables

Figures



Back

Close

Full Screen / Esc

Printer-friendly Version

Interactive Discussion



CO₂ exchange across
Northern Eurasia

M. A. Rawlins et al.

Title Page

Abstract

Introduction

Conclusions

References

Tables

Figures



Back

Close

Full Screen / Esc

Printer-friendly Version

Interactive Discussion

**Table 1.** Model participating in the Vulnerability of Permafrost Carbon Research Coordination Network (RCN) retrospective simulations. Modeling groups provided outputs over the time period listed for each model.

Model	Institution	Time Period
Community Land Model (CLM4.5)	National Center for Atmospheric Research, USA	1960–2004
Common Land Model (COLM)	Beijing Normal University, China	1960–2000
Interaction Sol-Biosphère-Atmosphère (ISBA)	National Centre for Meteorological Research, France	1960–2009
Joint UK Land Environment Simulator (JULES)	Met Office, UK	1960–2000
Lund-Potsdam-Jenna General Ecosystem Simulator (LPJG)	Lund University, Sweden	1960–2009
Model for Interdisciplinary Research on Climate, Earth System Model (MIROC)	Japan Agency for Marine-Earth Science and Technology, Japan	1960–2009
Organising Carbon and Hydrology In Dynamic Ecosystems (ORCHIDEE)	Institute Pierre Simon Laplace (IPSL), France	1960–2004
University of Victoria (UVic)	University of Victoria, Canada	1960–2009
Variable Infiltration Capacity (UW-VIC)	University of Washington, USA	1960–2006

CO₂ exchange across
Northern Eurasia

M. A. Rawlins et al.

Table 2. Properties in each model relevant to simulation of land–atmosphere CO₂ dynamics, particularly for the northern high latitude terrestrial biosphere. Properties are indicated as present (✓), absent (×) or otherwise (see footnote for details).

	CLM4.5	CoLM	ISBA	JULES	LPJG	MIROC	ORCHIDEE	UVic	UW-VIC
Light limitation	✓	✓	✓	✓	✓	✓	✓	✓	✓
N limitation	×	×	×	×	×	×	×	×	✓
CO ₂ fertilization	×	×	✓	✓	✓	×	×	×	×
Factors affecting R _h ^a	M + T + (C : N) + O ₂ ^e	M + T	M + T	M + T	M + T	M + T	M + T + C _{soil}	M + T	M + T
C _{soil} layered? (Depth?)	✓ (4 m)	× (3.4 m)	× (1 m)	implicit	implicit	implicit	✓ (2–47 m)	✓ (3.35 m)	×
Disturbance (F/L/I) ^c ?	F + L	F	×	×	F	F + L	×	L	×
Vegetation dynamic?	✓	✓	×	Vegetation dynamic?	✓	✓	×	✓	×
LAI ^d dynamic?	✓	✓	✓	✓	✓	×	✓	✓	×
LAI _{max} prescribed?	×	×	×	✓	×	✓	✓	×	×
Max veg height prescribed?	×	✓	✓	✓	×	✓	×	×	✓
Max rooting depth	variable	3.4 m	2 m	–	2 m	1 m	variable	3.35 m	1 m
Snow insulation type	multi-layer	multi-layer	multi-layer	multi-layer	implicit	multi-layer	implicit	–	bulk
Talik formation	✓	×	×	✓	×	✓	×	✓	✓

^a Heterotrophic respiration.^b Soil carbon.^c Fire; Land-use change; Insects.^d Leaf Area Index.^e Moisture; Temperature; Carbon/Nitrogen ratio; Oxygen.^f max height prescribed for shrubs.

Title Page

Abstract

Introduction

Conclusions

References

Tables

Figures

I ◀

▶ I

◀

▶

Back

Close

Full Screen / Esc

Printer-friendly Version

Interactive Discussion



CO₂ exchange across Northern Eurasia

M. A. Rawlins et al.

[Title Page](#)

[Abstract](#)

[Introduction](#)

[Conclusions](#)

[References](#)

[Tables](#)

[Figures](#)

[I◀](#)

[▶I](#)

[◀](#)

[▶](#)

[Back](#)

[Close](#)

[Full Screen / Esc](#)

[Printer-friendly Version](#)

[Interactive Discussion](#)



Table 3. Flux tower sites from the LaThuile dataset (Baldocchi, 2008) used in this study. Site Nur-Hakasija consists of records from 3 sub-sites which all fall within the same RCN model grid as shown by symbols in Fig. 4. GPP and ER in the La Thuile dataset are calculated using methodologies described in Reichstein et al. (2005).

Site	coordinates	IGBP class	start/end years
Chersky (CHE)	68.61° N, 161.34° E	mixed forest	2002–
Chokurdakh (COK)	70.62° N, 147.88° E	open shrubland	2003–2005
Nur-Hakasija (HAK)	54.77° N, 89.95° E	grassland	2002–2004
Zotino (ZOT)	60.80° N, 89.35° E	evergreen needleleaf forest	2002–

CO₂ exchange across Northern Eurasia

M. A. Rawlins et al.

Table 4. Average model error in $\text{gC m}^{-2} \text{month}^{-1}$ for site-level comparisons over the years 2002–2005 shown in Figs. 2–4. Errors are calculated as the average ($\hat{\epsilon}_j$) over all years and months for which a model estimate and site estimate are available at a given site. Thus for each site and month the error is calculated as the difference between the model and observed values: $\epsilon_j = C_j - C_{\text{obs}}$, where C_j is GPP, ER or NEP for model j and C_{obs} is the observed value from the La Thuile FLUXNET observations (Baldocchi, 2008). Model estimates for years 2002–2005 are not available for CoLM and JULES. Differences were evaluated using a 2-way repeated measures ANOVA test. Test design was a comparison of GPP vs ER t tests for (i) each area separately; (ii) GPP and ER pooled for the the two tundra sites and across the two forest sites; and (iii) GPP errors pooled across the four sites vs. ER pooled across the four sites.

Model	CHE			COK			HAK			ZOT		
	GPP	ER	NEP	GPP	ER	NEP	GPP	ER	NEP	GPP	ER	NEP
MOD17	-2	-	-	-11	-	-	13	-	-	10	-	-
CLM4.5	-25	-19	-6	-42	-23	-19	8	22	-15	78	81	-3
ISBA	27	25	2	34	41	-7	82	78	3	82	98	-16
LPJG	-10	-5	-5	-5	-1	-4	53	74	-22	-34	-13	-20
MIROC	20	18	2	49	43	6	28	37	-10	-4	21	-25
IPSL	23	12	11	49	32	17	16	21	-6	-30	-6	-24
UVic	-14	-7	-7	16	36	-20	30	38	-9	-7	31	-38
UW-VIC	27	34	-6	140	119	19	18	33	-16	2	20	-18
mean	7	8	-1	34	35	-1	34	43	-11	13	33	-20

Title Page

Abstract

Introduction

Conclusions

References

Tables

Figures

I ◀

▶ I

◀

▶

Back

Close

Full Screen / Esc

Printer-friendly Version

Interactive Discussion



CO₂ exchange across Northern Eurasia

M. A. Rawlins et al.

Title Page

Abstract

Introduction

Conclusions

References

Tables

Figures

◀

▶

◀

▶

Back

Close

Full Screen / Esc

Printer-friendly Version

Interactive Discussion



Table 5. Trend in GPP, ER, and NEP over simulation period for each model. Trend slopes ($\text{gC m}^{-2} \text{yr}^{-2}$) are estimated using an auto-regressive AR[1] model to account for temporal autocorrelation. Standard error for the regression is indicated in (). SD of the model means is shown in []. Significant trends ($p < 0.01$) are denoted with an asterisk (*).

Model	GPP	ER	NEP
CLM4.5	1.3*(0.18)	1.0*(0.15)	0.27*(0.06)
CoLM	1.3*(0.19)	0.9*(0.18)	0.31*(0.07)
ISBA	3.9*(0.29)	3.1*(0.23)	0.78*(0.11)
JULES	1.7(0.27)	1.3(0.19)	0.33*(0.11)
LPJG	1.2*(0.11)	1.0*(0.11)	0.17*(0.06)
MIROC	1.9*(0.16)	1.7*(0.15)	0.24*(0.12)
ORCHIDEE	1.6*(0.15)	1.1*(0.13)	0.43*(0.08)
UVic	1.7*(0.18)	1.6*(0.18)	0.11(0.06)
UW-VIC	1.4*(0.12)	1.4*(0.13)	0.02(0.05)
mean	1.8[0.78]	1.5[0.64]	0.29[0.18]

CO₂ exchange across
Northern Eurasia

M. A. Rawlins et al.

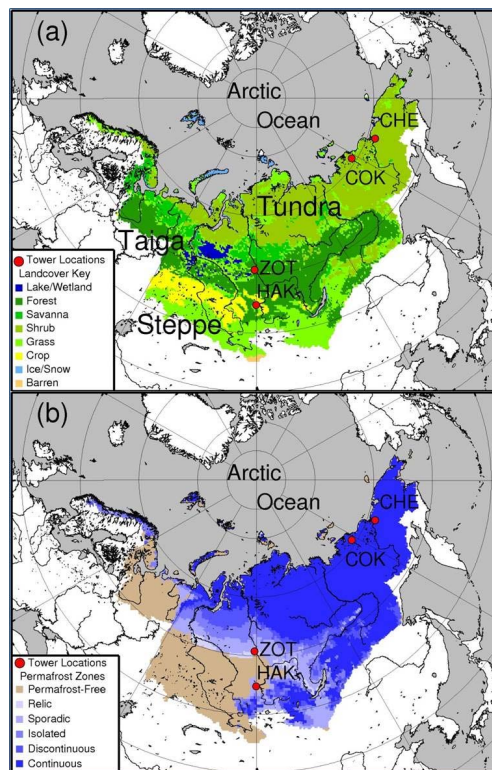


Figure 1. Study domain spanning the arctic drainage basin in northern Eurasia. Map panels show **(a)** plant functional types (PFTs) and **(b)** permafrost classification along with tower sites used in the study: **(a)** Chersky, **(b)** Chokurdakh, **(c)** Nur-Hakasija, and **(d)** Zotino (Table 3). Gridded PFTs are from the MODIS MOD12 product (Oak Ridge National Laboratory, 2014). Permafrost classes for each grid are drawn from the CAPS dataset (International Permafrost Association Standing Committee on Data Information and Communication, 2003).

Title Page

Abstract

Introduction

Conclusions

References

Tables

Figures

◀

▶

◀

▶

Back

Close

Full Screen / Esc

Printer-friendly Version

Interactive Discussion



CO₂ exchange across
Northern Eurasia

M. A. Rawlins et al.

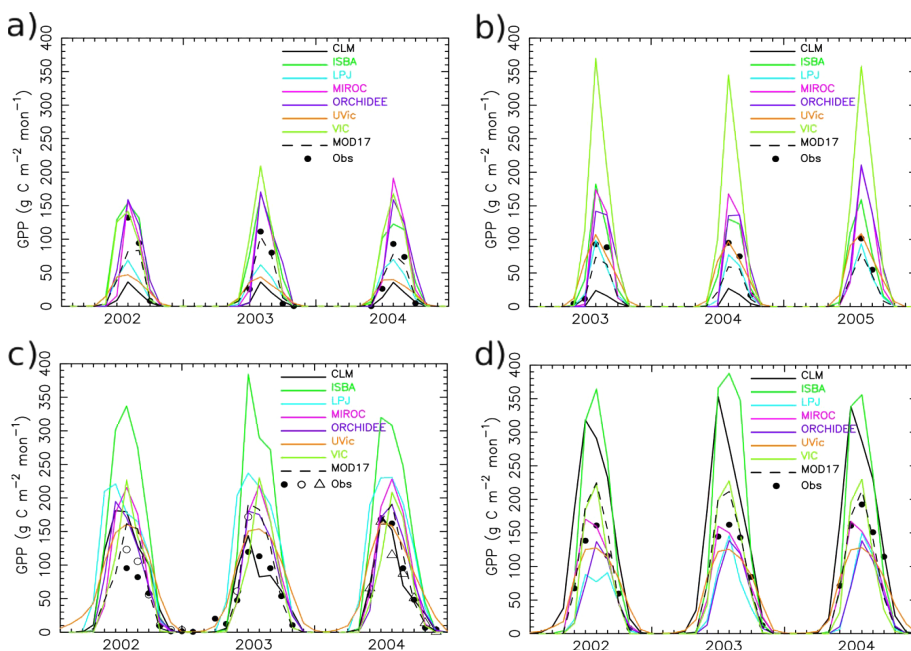


Figure 2. Monthly GPP at sites **(a)** Chersky, **(b)** Chokurdakh, **(c)** Nur-Hakasija, and **(d)** Zotino (Obs, Table 3). Colored lines trace monthly GPP for each model grid that encompassing the tower location. Site Nur-Hakasija includes research areas Ha1 (filled circle), Ha2 (open circle), and Ha3 (triangle).

[Title Page](#)
[Abstract](#)
[Introduction](#)
[Conclusions](#)
[References](#)
[Tables](#)
[Figures](#)
[◀](#)
[▶](#)
[◀](#)
[▶](#)
[Back](#)
[Close](#)
[Full Screen / Esc](#)
[Printer-friendly Version](#)
[Interactive Discussion](#)


CO₂ exchange across Northern Eurasia

M. A. Rawlins et al.

Title Page

Abstract

Introduction

Conclusions

References

Tables

Figures



Back

Close

Full Screen / Esc

Printer-friendly Version

Interactive Discussion

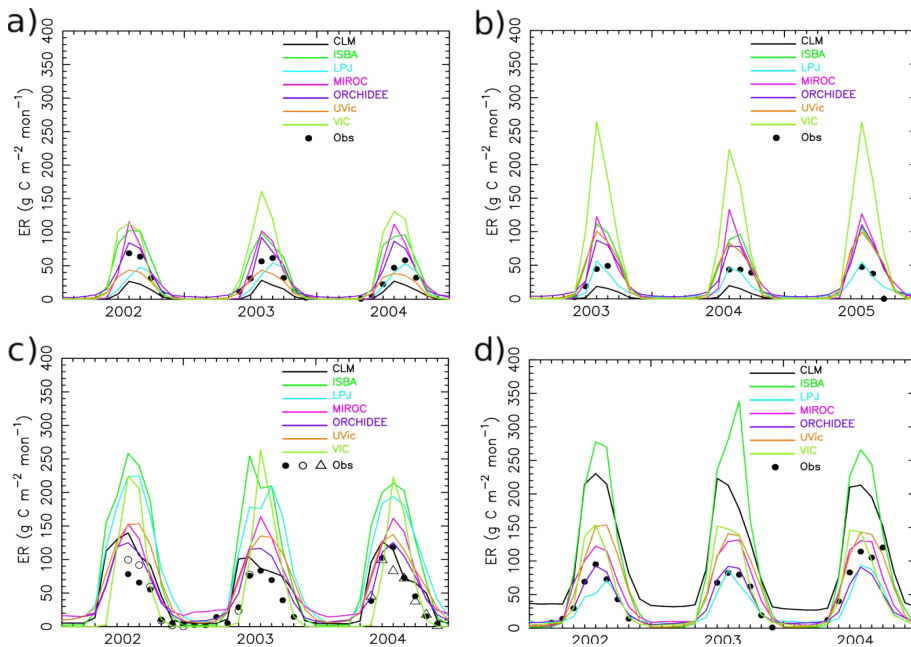


Figure 3. As in Fig. 2, for ER.

CO₂ exchange across
Northern Eurasia

M. A. Rawlins et al.

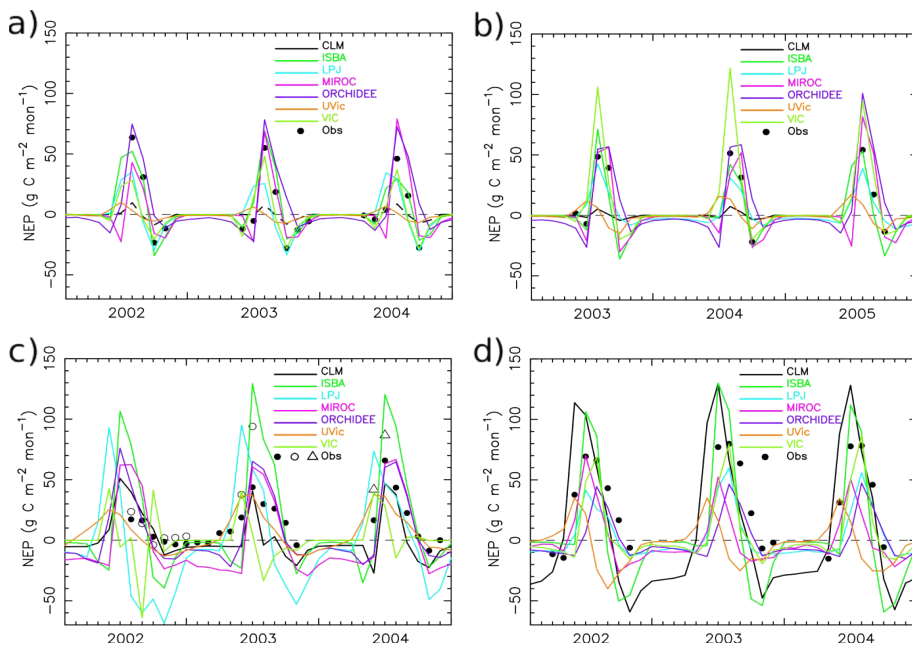


Figure 4. As in Fig. 2, for NEP. NEP = GPP – ER.

[Title Page](#)
[Abstract](#)
[Introduction](#)
[Conclusions](#)
[References](#)
[Tables](#)
[Figures](#)

[Back](#)
[Close](#)
[Full Screen / Esc](#)
[Printer-friendly Version](#)
[Interactive Discussion](#)


CO₂ exchange across
Northern Eurasia

M. A. Rawlins et al.

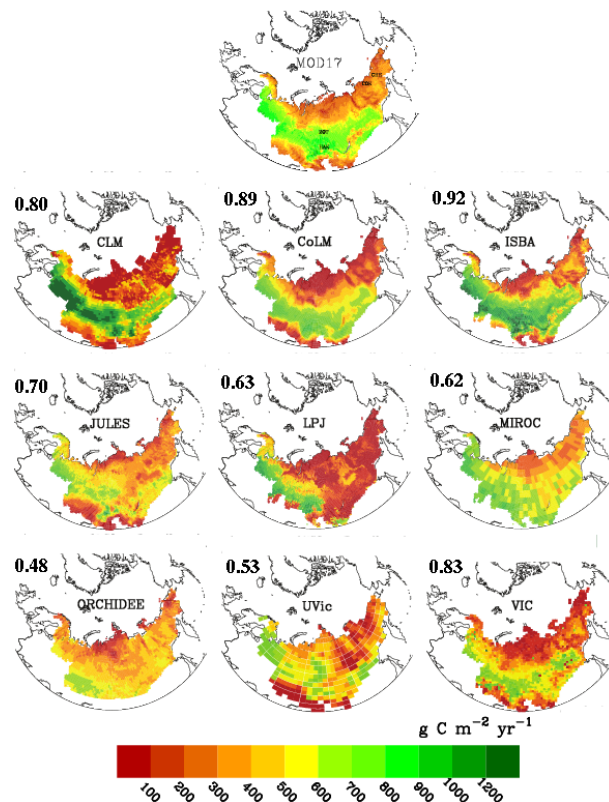


Figure 5. Mean annual Gross Primary Productivity (GPP) from the permafrost RCN models and from the MOD17 product. The averaging period is 2000–2009 for GPP from the MOD17 product and all models with the exception of CLM4.5 (1995–2004); CoLM (1991–2000); and JULES (1991–2000). Spatial correlations between MOD17 GPP and each model GPP for all grids is shown at upper left in each map panel.

Title Page

Abstract

Introduction

Conclusions

References

Tables

Figures

I ◀

▶ I

◀

▶

Back

Close

Full Screen / Esc

Printer-friendly Version

Interactive Discussion



CO₂ exchange across Northern Eurasia

M. A. Rawlins et al.

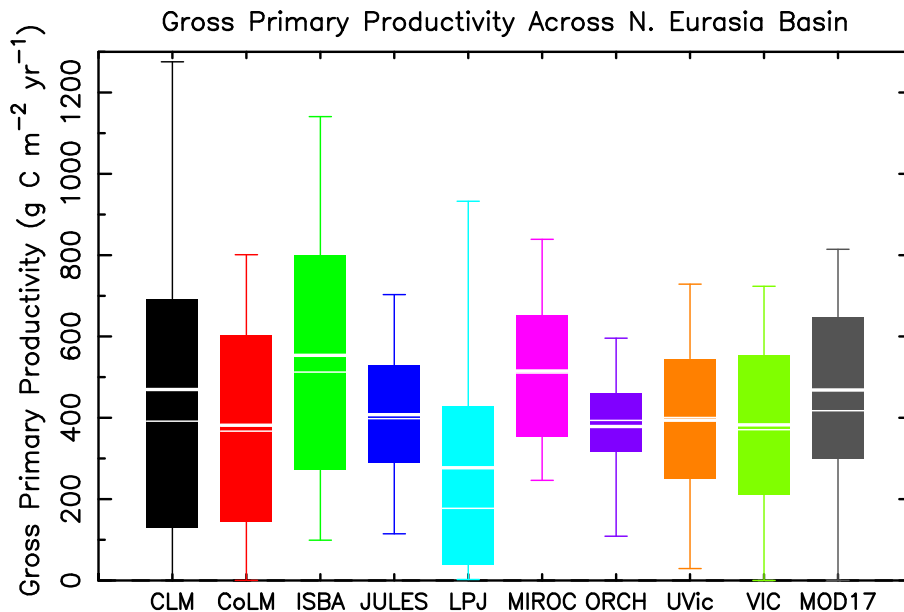


Figure 6. Distributions for mean annual GPP from the models and the MOD17 product over the averaging period listed in Fig. 5. The rectangles bracket the 25th and 75th percentiles. Whiskers extend to the 5th and 95th percentiles. Thick and thin horizontal lines mark the mean and median respectively.

Title Page

Abstract

Introduction

Conclusions

References

Tables

Figures

◀

▶

◀

▶

Back

Close

Full Screen / Esc

Printer-friendly Version

Interactive Discussion



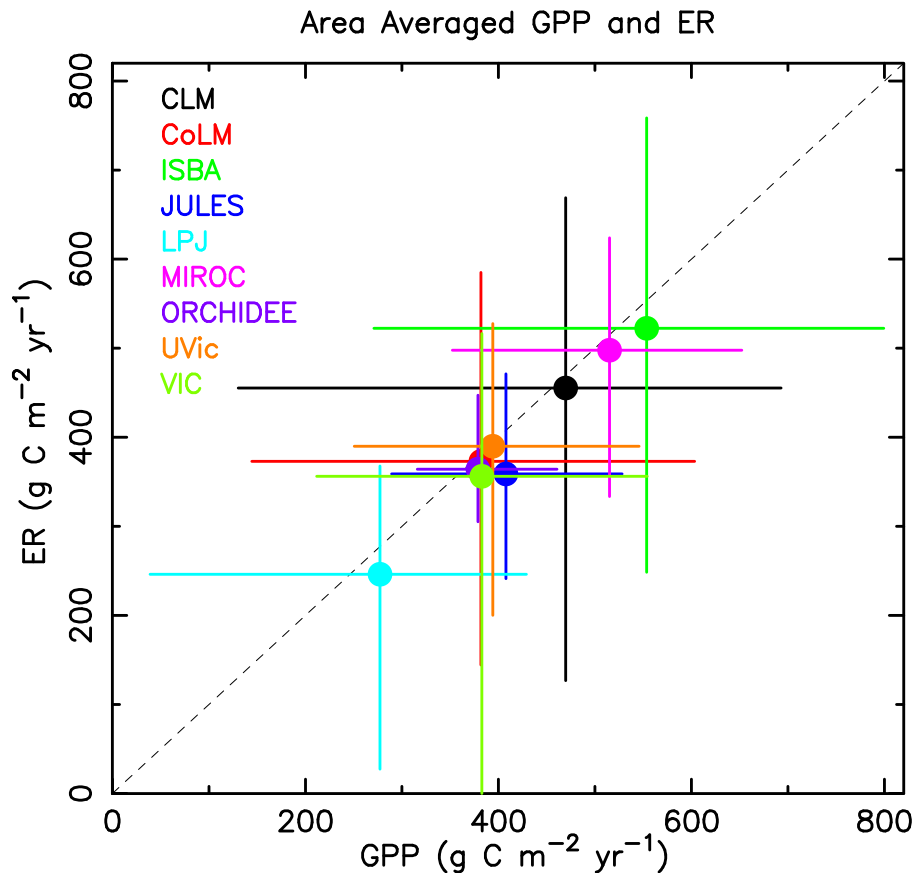


Figure 7. Spatially averaged ER vs. GPP over the period 1960–2009. Horizontal and vertical lines span the range across the 5th and 75th percentiles for GPP and ER, respectively. The GPP 5th and 75th percentiles are shown in Fig. 6. NEP is equal to the difference GPP minus ER.

Title Page

Abstract

Introduction

Conclusions

References

Tables

Figures



Back

Close

Full Screen / Esc

Printer-friendly Version

Interactive Discussion



CO₂ exchange across Northern Eurasia

M. A. Rawlins et al.

Title Page

Abstract

Introduction

Conclusions

References

Tables

Figures

◀

▶

◀

▶

Back

Close

Full Screen / Esc

Printer-friendly Version

Interactive Discussion

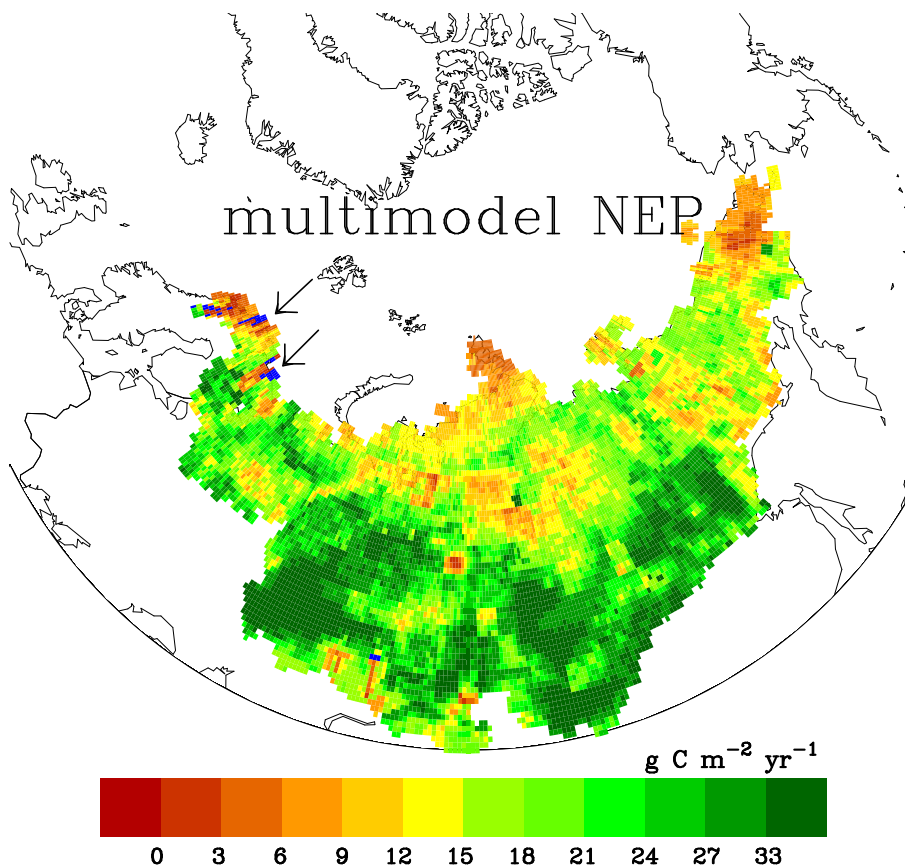


Figure 8. Annual NEP (1960–2009) averaged across the nine models. Areas in blue are a net annual source of CO₂. Arrows indicate the two source regions of CO₂ in Scandinavia.

CO₂ exchange across Northern Eurasia

M. A. Rawlins et al.

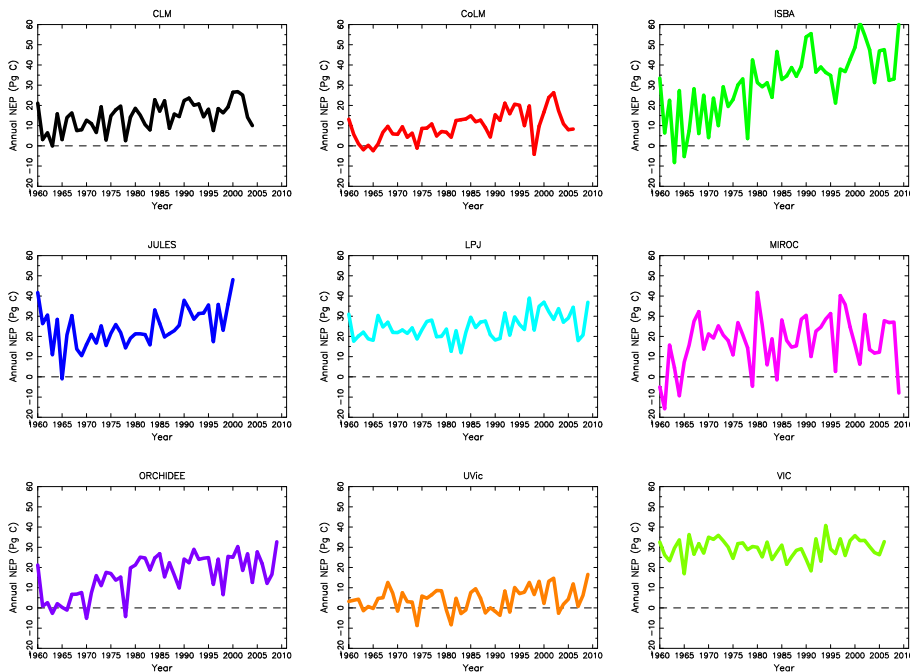


Figure 9. Spatially averaged annual NEP across the region, 1960–2009.

[Title Page](#)

Abstract	Introduction
Conclusions	References
Tables	Figures

◀
▶

◀
▶

[Back](#)
[Close](#)

[Full Screen / Esc](#)

[Printer-friendly Version](#)

[Interactive Discussion](#)



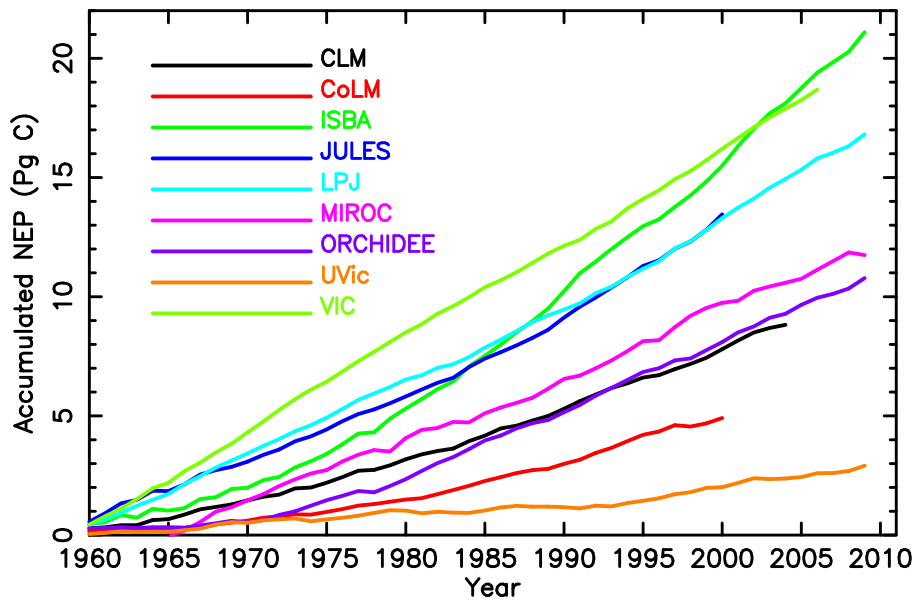


Figure 10. Cumulative NEP in PgC over the period 1960–2009.

CO₂ exchange across Northern Eurasia

M. A. Rawlins et al.

[Title Page](#)

[Abstract](#) | [Introduction](#)

[Conclusions](#) | [References](#)

[Tables](#) | [Figures](#)

[I ◀](#) | [▶ I](#)

[◀](#) | [▶](#)

[Back](#) | [Close](#)

[Full Screen / Esc](#)

[Printer-friendly Version](#)

[Interactive Discussion](#)



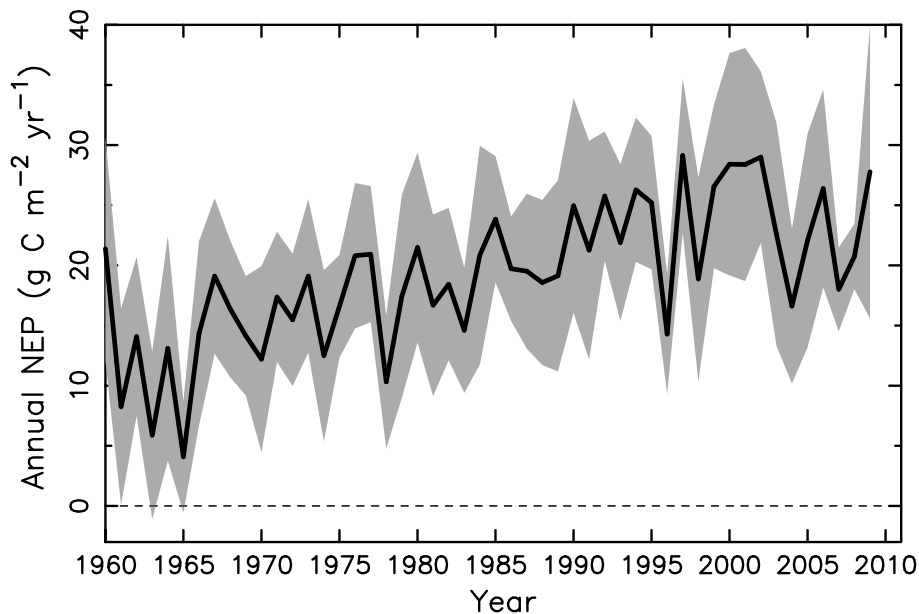


Figure 11. Spatially averaged annual NEP averaged across the nine models. Gray region marks the 95th confidence interval, where $CI = \mu \pm (SE \times 1.96)$, where μ is the nine model mean and SE is the standard error. SD (σ) used to estimate SE is obtained each year from the set of nine model NEP values used to obtain the yearly mean.

CO₂ exchange across Northern Eurasia

M. A. Rawlins et al.

[Title Page](#)

[Abstract](#) [Introduction](#)

[Conclusions](#) [References](#)

[Tables](#) [Figures](#)

[◀](#) [▶](#)

[◀](#) [▶](#)

[Back](#) [Close](#)

[Full Screen / Esc](#)

[Printer-friendly Version](#)

[Interactive Discussion](#)



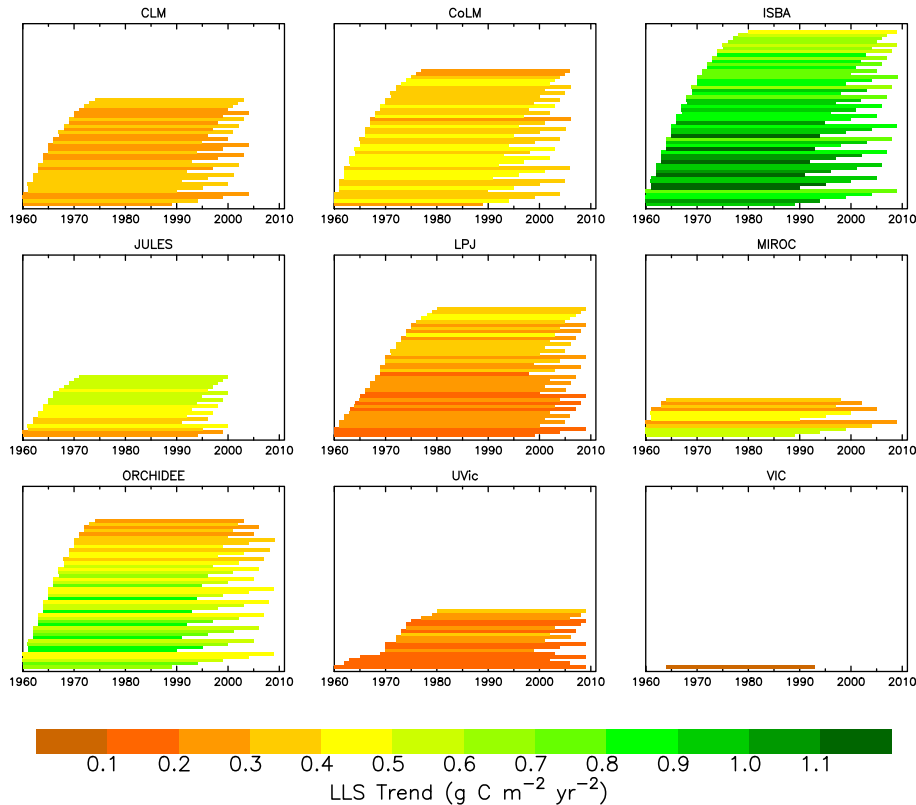


Figure 12. Magnitude of linear trend in NEP over given time interval for all trends significant at $p < 0.05$. All time intervals with a minimum of 20 yr and up to the full 1960–2009 period are sampled and each interval with a significant trend is then plotted. Thus each colored line represents a period for which the trend slope is significant. The color of the line and the period length is given by the length of the line, with start and end of line marking the start and end of the time interval.

Title Page

Abstract

Introduction

Conclusions

References

Tables

Figures

◀

▶

◀

▶

Back

Close

Full Screen / Esc

Printer-friendly Version

Interactive Discussion



CO₂ exchange across Northern Eurasia

M. A. Rawlins et al.

Title Page

Abstract

Introduction

Conclusions

References

Tables

Figures



Back

Close

Full Screen / Esc

Printer-friendly Version

Interactive Discussion

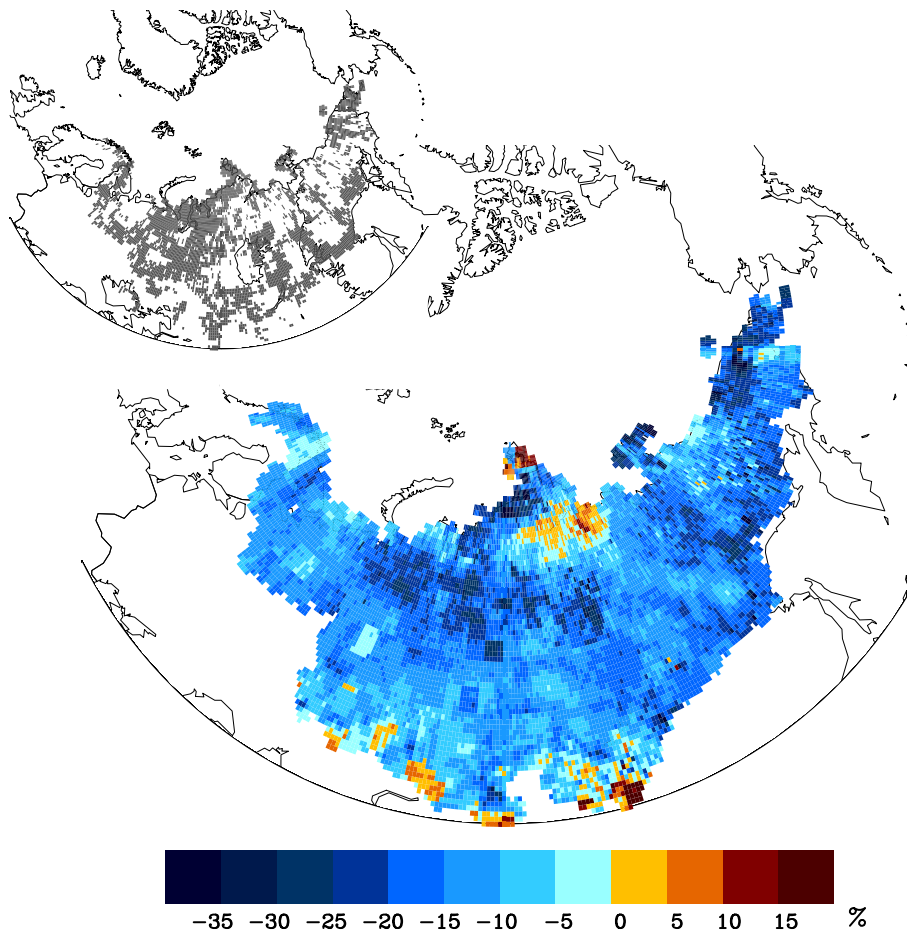


Figure 13. Change in soil organic carbon (SOC) residence time (RT) averaged across all nine models. Inset shows grids where residence time trend is significant for at least six of the nine models.